Emiliania huxleyi cultures as insights into palaeoceanographic proxies and processes

Thesis submitted in accordance with the requirements of the University of Liverpool for the degree of Doctor of Philosophy by

Samuel R Fielding

September 2010

Abstract

Estimating past oceanographic and atmospheric conditions and their interactions can help further understand the evolution of the Earth's climate system. In turn, this knowledge underlies the prediction of future climatic change. This thesis addresses questions regarding the reconstruction of past climatic variables such as sea-surface salinity and past climatic processes such as sulphate aerosol production. Each chapter uses novel or literature-derived data generated by culture experiments on the coccolithophorid alga *Emiliania huxleyi*. Analysis of these data provides caveats and improved parameter estimates for reconstructing past climatic variables and processes.

Analysis of *E. huxleyi* coccolith morphology as a palaeo-sea-surface salinity proxy using culture experiments and scanning electron microscopy demonstrates that while the proxy is stable in the open-ocean, populations from isolated and marginal settings such as Norwegian coastal waters display different characteristics. Therefore, it is recommended that the palaeosalinity proxy should be re-calibrated for application in these isolated and marginal settings. However, analysis of *E. huxleyi* cellular morphology data from the literature does not demonstrate a similar biogeographical divide. Nevertheless, these data provide an improved estimate of the size range of *E. huxleyi* cells for use in reconstructing palaeo-sea-surface CO_2 in combination with alkenone carbon isotope measurements. This updated estimate introduces additional errors into palaeo-CO_2 reconstruction using this method which are approximately double those made previously.

A Rayleigh distillation model highlights *E. huxleyi* bloom formation as a potential mechanism for causing part of the variation in coccolith Sr/Ca that is observed in the modern ocean and in the sedimentary record. This proposed mechanism exists in addition to coccolith calcification rate and temperature which are thought to be the primary factors controlling coccolith Sr/Ca. However, these results still support the use of coccolith Sr/Ca as a qualitative palaeoproductivity proxy.

E. huxleyi growth rate data compiled from the literature demonstrate that the relationship between growth rate and temperature follows a power function. This species-specific relationship allows models of *E. huxleyi* bloom formation to be calculated with greater accuracy. This is in contrast to previous estimates of growth rate as a function of temperature which assumed an exponential relationship based on data from multiple species.

The relationship between sea-surface salinity and *E. huxleyi* dimethylsulphoniopropionate (DMSP) production is quantified using gas-chromatograph analysis of culture samples. These data suggest an increase in *E. huxleyi* DMSP at higher salinities as has been observed in other algal species. Results predict increased DMSP as a result of salinity change at the Last Glacial Maximum in all ocean regions except for the North Atlantic. These conclusions are partly reflected by records of sulphate deposition in ice cores from both Greenland and Antarctica.

Contents

Acknowledgements

I would like to thank my supervisors Jens Herrle, David Montagnes, and Richard Worden for their continued support and friendship along the way.

Additionally I am also indebted to the following:

Michael Steinke for analysing the DMS/DMSP samples.

The large team of technical support staff for each doing their bit to help. Alphabetically you are: Sabena Blackbird, Julie Clark, Evelyn Connell, Greg Flattery, Gregor Govan, Tom Heyes, Paula Houghton, Peter Jones, Paul Loughnane, Sravan-Raju Pandalaneni, Carmel Pinnington, Anu Thompson, Cornelis Veltkamp, Jean Wood, and Carl Wright.

Kostas Kiriakoulakis, Claire Mahaffey, Pascal Salaun, Ric Williams, and George Wolff for their helpful discussion.

The assorted biologists and earth scientists I've got to know for the camaraderie and for their sharing in many an adventure. Chronologically starting with Jan and Big Dave and ending with whoever might be the latest addition.

Finally, I am forever indebted to Laura for putting up with me for so long and for supporting me while I wrote this.

1 General Introduction

1.1 Palaeoceanographic proxies and processes

Knowledge of past oceanographic and atmospheric conditions and their interactions is key to understanding the how the Earth's climate system might develop in the future. Ascertaining the interaction of past oceanographic and atmospheric conditions relies on understanding driving mechanisms and in being able to reconstruct past environmental variables such as sea-surface temperature (SST), sea-surface salinity (SSS), productivity, and atmospheric CO_2 concentration.

One way in which past environmental variables can be estimated is by proxy-reconstruction (Wefer et al. 1999). This is achieved by converting a measurable variable (proxy) from a section of sediment to an estimate of an environmental variable (e.g. temperature or salinity), when the sediment was deposited. This estimate is made based on a quantified relationship between proxy variable and environmental variable from the present ocean. Therefore, palaeoceanographic reconstruction consists of two distinct phases: i) determining a reliable relationship between proxy and environmental variable and ii) measuring the proxy variable in the sedimentary record.

Additionally, the potential interaction of palaeoceanographic processes with palaeoclimate may be understood by quantifying mechanisms which are known to have an effect in the present ocean – atmosphere system. For example, the relationship between the sulphide compound dimethylsulphide (DMS) being released from the upper ocean and cloud formation has been extensively researched as a potential driver of palaeoclimate since the inception of the hypothesis more than twenty years ago (Charlson et al. 1987).

Understanding of such mechanisms can come from empirical oceanographic measurements, laboratory experiments, and from mathematical modelling.

This thesis will focus on i) improving the reliability of relationships between proxies and environmental variables and ii) quantifying a mechanism of potential ocean – atmosphere interaction. Specifically this thesis aims to address a subset of proxies and mechanisms which relate to the marine algal species *Emiliania huxleyi*, the nature of which are now discussed.

1.2 Proxies and processes based on *E. huxleyi*

1.2.1 *E. huxleyi*-based proxies

E. huxleyi is a unicellular marine photosynthetic algae with a global distribution (Paasche 2002). As such it grows in the upper several hundred metres of the ocean where there is enough light for photosynthesis (the photic zone). However, *E. huxleyi* cells eventually sink out of the photic zone and are ultimately incorporated into sediments on the ocean floor. Therefore, characteristics of *E. huxleyi*, such as its morphology and chemical composition which are determined in the upper ocean, are preserved in the sediment record.

E. huxleyi leaves both inorganic and organic traces in the sediment record which both provide several opportunities for palaeoceanographic proxy development (Bijma et al. 2001; Bollmann and Herrle 2007; Muller et al. 1998; Stoll and Ziveri 2004). Above the calcite compensation depth the inorganic remains of *E. huxleyi* in the sediments come in the form of calcite platelets known as coccoliths. These are produced during the lifetime of the cell and surround the cell to form what is known as the coccosphere. The organic

sedimentary traces remaining from cell growth in the photic zone are primarily long chain (C_{37}) alkenones (methyl ketones). As *E. huxleyi* is present in abundance in the present ocean (Paasche 2002), the relationship between the chemistry and morphology of both its alkenones and its coccoliths and the environmental conditions in which it grows can be quantified.

The use of coccolith morphology as a proxy for SSS (Bollmann and Herrle 2007; Bollmann et al. 2009) is relatively new. Palaeo-SSS can be reconstructed from the relationship between SSS and the dimensions of coccoliths from the present ocean as determined by scanning electron microscopy (SEM). The ratio of strontium to calcium (Sr/Ca) in coccoliths of *E. huxleyi* and other coccolithophores has been correlated to calcification rate in laboratory experiments (Stoll et al. 2002a; Stoll et al. 2002b) and is therefore thought to be an indicator of coccolithophore productivity. The magnesium/calcium ratio (Mg/Ca) of foraminiferal calcite has long been used as a palaeo-SST proxy but the use of coccolithophore Mg/Ca in the same way has not been viable due to problems with sample cleaning (Stoll et al. 2001).

A proxy based on the ratios between $C_{37:2}$, $C_{37:3}$, and $C_{37:4}$ alkenones (U^K_{37}) (Conte et al. 2006; Prahl and Wakeham 1987) has been commonly used to reconstruct palaeo-SST (e.g. Sikes et al. 2009). Additionally, the carbon isotope composition of $C_{37:2}$ alkenones has been used to reconstruct both coccolithophore growth rate and sea-surface dissolved CO_2 concentrations (Henderiks and Pagani 2007; Pagani et al. 2005).

1.2.2 Why is *E. huxleyi* useful as a proxy generator?

A primary reason for the use of proxies based on *E. huxleyi* is its wide geographical distribution and abundance. *E. huxleyi* is found in all parts of the modern ocean (Hegseth

and Sundfjord 2008; Paasche 2002) except perhaps from extreme high latitude Antarctic waters (Gravalosa et al. 2008; Mohan et al. 2008), despite having been recorded from periantarctic basins such as the Weddell, Ross, and Bellingshausen seas in the late Quaternary (Villa et al. 2005). Further, *E. huxleyi* is the most numerous coccolithophore in the modern ocean (Paasche 2002). As a result, *E. huxleyi*-based proxies can be consistently applied over a large geographical scale. Second, *E. huxleyi* has been present in the sedimentary record for the last ~268 kyr and has been the dominant coccolithophore species since between ~70 and ~80 kyr ago (Thierstein et al. 1977). This timeframe therefore allows *E. huxleyi*-based proxies to be applied to questions about recent glacial-interglacial cycles. Third, the small size (~5-10 μm diameter) of *E. huxleyi*, combined with its abundance, allows for very high resolution analysis of sediments compared to larger organisms such as foraminifera (often up to 1000 μm).

One notable characteristic of *E. huxleyi* is its ability to form blooms covering up to ~1,000,000 km^2 (Raitsos et al. 2006) and containing higher than background concentrations of cells and coccoliths (Balch et al. 1996b; Berge 1962). These seasonal events are likely to contribute a significant proportion of the *E. huxleyi* traces in the sediments. As such, understanding patterns of past bloom occurrence is important for interpreting *E. huxleyi*-based proxy signals (Bijma et al. 2001).

1.2.3 *E. huxleyi* as a driver of processes

The chemical properties of ocean surface waters are key to the exchange (outgassing and dissolution) of elements such as C, N, and S between ocean and atmosphere and are therefore an important link in the regulation of global biogeochemical cycles (Andreae and Crutzen 1997; Raven and Falkowski 1999). The abundance of photosynthetic algae in the photic zone makes them important contributors to the chemical

composition of the ocean's surface. While chemical composition of algae varies widely, coccolithophores such as *E. huxleyi* are notable for two reasons. First, coccolithophores produce both organic carbon (sugars, proteins, and lipids) and inorganic carbon (calcite). The balance of the reactions converting dissolved carbon species in seawater to organic carbon and calcite is important for determining the carbonate system, and therefore the capacity of the ocean to absorb or lose CO_2 to the atmosphere (Zeebe and Wolf-Gladrow 2001). Second, coccolithophores synthesise larger quantities per cell of the sulphur compound dimethylsulphoniopropionate (DMSP) than other algal groups (Malin and Steinke 2004). DMSP is the precursor to DMS, which can dissolve in seawater and escape to the atmosphere, ultimately reacting to form sulphate aerosols. These sulphate aerosols have the potential to trigger cloud formation and to scatter incoming solar radiation, thus having a net climatic cooling effect (Simo 2001).

1.3 Aims and concepts for this thesis

Understanding of palaeoceanographic proxies and processes is still being developed. In some cases the relationships between *E. huxleyi* chemistry and morphology and environmental parameters have only been derived from a limited subset of environmental scenarios, and therefore require further validation. In this thesis, data from *E. huxleyi* culture experiments are used to test current hypotheses regarding these relationships.

E. huxleyi is easy to isolate and grow under laboratory conditions in comparison to most other coccolithophores and therefore *E. huxleyi* cultures are a popular analytical tool (Probert and Houdan 2004). Data generated by culture experiments have several

advantages over *in situ* (i.e. oceanographic) data collection. First, cultures allow specific hypotheses to be tested. This is primarily achieved through the experimental control of most, if not all, major environmental parameters. For example, to test for a relationship between salinity and coccolith size (*see* Chapter 2), variables such as temperature, light intensity, nutrient supply and genotype can be kept constant while only salinity is varied. Second, culture experiments provide a relatively inexpensive and fast method of obtaining data compared to an *in situ* approach. As a result, there are a large number of well constrained literature data available for analysis.

As such, this thesis relies on *E. huxleyi* cultures as either, i) a method of controlling variables (Chapters 2, 4, and 6) or ii) a method of obtaining a much larger quantity of data than would otherwise be possible (Chapters 2, 3, and 5).

1.4 Structure of chapters

Chapter 2—Presents original experimental culture data examining the relationship between salinity and *E. huxleyi* coccolith morphology (used for palaeo-sea-surface salinity (SSS) reconstruction). These new data are synthesised with those from the literature and implications for palaeo-SSS reconstruction are discussed.

Chapter 3—Presents a meta-analysis of size estimates of *E. huxleyi* cells from literature experimental culture data. This chapter also discusses the implications for reconstruction of palaeo-sea-surface aqueous CO_2 concentration which uses *E. huxleyi* cell size as an input variable.

Chapter 4—Uses experimental culture data from the literature on Sr incorporation into coccolith calcite to estimate the effect of *E. huxleyi* bloom formation on coccolith

Sr/Ca based on a Rayleigh distillation model. Implications for the reconstruction of coccolithophore palaeoproductivity using Sr/Ca as a proxy are discussed.

Chapter 5—Presents a meta-analysis of *E. huxleyi* growth rate in response to temperature from literature experimental culture data. Additionally, this chapter provides improved estimates of this growth rate – temperature response to be used as an input variable in oceanographic models of *E. huxleyi* bloom formation.

Chapter 6—Presents original experimental culture data examining the effect of salinity on the production of DMSP, the precursor to climatically important sulphate aerosols. Implications for biogenic DMSP production at the Last Glacial Maximum (LGM) are discussed.

Chapter 2 is based on a published manuscript ((Fielding et al. 2009) *see* Appendices). All other chapters are presented in the form in which they are to be submitted for publication. Chapters 3 and 4 are to be submitted to *Paleoceanography*, Chapters 5 and 6 are to be submitted to *Limnology & Oceanography*.

2 Assessing the applicability of *Emiliania huxleyi* coccolith morphology as a sea-surface salinity proxy

2.1 Abstract

Culture experiments were used to assess the applicability of *Emiliania huxleyi* coccolith morphology as a palaeo-sea surface salinity (SSS) proxy. Coccolith morphology was dependent on salinity over a range reflecting present day marine conditions; both coccolith size and the number of coccolith elements increased linearly with increasing salinity. Using regression analysis, the effect of salinity on coccolith morphology was compared to those previously observed in sediment core-top and plankton data. No significant differences were found between the slopes of these data, suggesting that salinity is the primary control on *E. huxleyi* coccolith size and element number in the ocean. However, the intercepts of the culture data were significantly higher. A combination of experimental and literature analysis indicated that temperature and nutrients were unlikely to be the causes of this discrepancy. Literature analysis also highlighted that coccolith size data from marginal environments displayed different intercepts to those from the open ocean data. This suggests that discrete morphotypes exist in these marginal locations. It is therefore recommended that the original *E. huxleyi* coccolith morphology palaeo-SSS transfer function requires further evaluation before being routinely applied.

2.2 Introduction

The ability to reconstruct historical sea-surface salinity (SSS) patterns is essential to understanding past ocean circulation and climatic change (Hay 2008; Hay et al. 2006). However, unlike temperature, palaeo-SSS still cannot be reconstructed with reliability using either oxygen isotope residuals (Rohling 2000; Rohling 2007; Schmidt 1999) or dinoflagellate cyst morphology (De Vernal et al. 2001). As a step towards addressing this problem, recent studies (Bollmann and Herrle 2007) have indicated that the morphology of external calcite plates (coccoliths) of the ubiquitous and abundant coccolithophorid *Emiliania huxleyi* may provide a useful proxy with which to reconstruct SSS. Analysis of sediment core-top samples (approximately Holocene in age) has revealed that *E. huxleyi* coccolith size is linearly related to present annual mean SSS between 33 and 39, though the relationship deviated from linear outside this range (Bollmann and Herrle 2007). Further, a linear relationship between coccolith size and in situ SSS (32 – 39) has been demonstrated for *E. huxleyi* plankton samples (Bollmann et al. 2009). Correlations between ocean SSS and coccolith morphology are encouraging for the use of coccoliths as a proxy for palaeo-SSS reconstructions. However, a direct relationship needs to be established between salinity and *E. huxleyi* coccolith morphology under controlled laboratory conditions to assess the robustness of such a proxy. To date, culture studies have indicated that reduced salinity (14 – 34) affects coccolith morphology in some strains of *E. huxleyi* (Green et al. 1998; Paasche et al. 1996). However, the limited number of salinity treatments makes the quantification of this relationship difficult. Further, the limited overlap between previous experimental measurements and the present SSS range (mostly between 33 and 38) precludes comparison of this effect with data from environmental samples.

In this study coccolith morphology is assessed using *E. huxleyi* cultures grown in the laboratory over a broad range of salinities (26 – 41). As temperature may also affect coccolith morphology (Watabe and Wilbur 1966), the effect of temperatures between 10°C and 20°C on coccolith size is also tested. Finally, these laboratory-based measurements of the coccolith morphology vs. salinity relationship are explicitly compared with those made from sediment core-top and plankton samples to establish whether a consistent trend between morphology and salinity occurs. In this way the general applicability of *E. huxleyi* coccolith morphology as a proxy for palaeo-SSS is assessed. This analysis reveals a direct relationship between coccolith morphology and salinity consistent with observations from sediment core-top and plankton samples. However, there were differences between the intercepts of the experimentally derived coccolith morphology vs. salinity relationships and those for the environmental samples, and potential environmental and geographic reasons for these inconsistencies are discussed.

2.3 Methods

2.3.1 Culturing and morphological analysis

Emiliania huxleyi strain PLY B92/11 (isolated from Bergen Fjord, W. Norway) was grown in semi-continuous batch culture (Brand et al. 1981) in borosilicate glass tubes (13 mm diam.) each filled with 15 mL of artificial sea water (ASW) at ~30 μmol photons m^{-2} s^{-1} (broadly representative for natural *E. huxleyi* growth conditions, (Cortes et al. 2001; Kirk 1994) continuous light (Philips TL-D/865 Super 80). The use of continuous light ensured cultures did not undergo synchronised division, which could bias results (Muller et al. 2008). ASW was made using deionised water, 0.5 g Tricine L^{-1} (Sigma, T-0377) to

prevent precipitation of salts during autoclaving, and variable concentrations of synthetic sea salt (Ultramarine, Waterlife Research Industries). After autoclaving, f/2 enrichment media was added (Sigma, G0154; (Guillard 1975)). Salinities were determined using an Autosal 8400 (Guildline Instruments).

Cultures were grown at 10 salinities (between 18 and 41) and at four temperatures (between 10°C and 20°C). One culture was acclimated to each treatment for >10 generations (as determined by light microscopy cell counts – *see* Appendix 2.1). Throughout acclimation and subsequent experimentation, cultures were mixed twice daily and maintained in exponential growth phase at cell concentrations below 3.0×10^4 cells mL^{-1}. Acclimated specific growth rates were between 0.05 and 0.7 d^{-1} (salinity gradient) and 0.2 and 0.95 d^{-1} (temperature gradient). In mid-exponential phase, one sample from each treatment was taken for coccolith morphological analysis using a scanning electron microscope (SEM). Samples were filtered onto a polycarbonate filter (0.4 μm pore size), rinsed in NH_4OH-buffered H_2O (pH 8.5), mounted on stubs, and sputter-coated with ~15 nm of gold-palladium. Cultures grown below a salinity of 26 failed to produce sufficient coccoliths and were excluded from analysis.

Images were captured using a Philips XL30 SEM on 30 detached, flat-lying coccoliths per sample. Length and width of both the coccolith distal shield (DL and DW, respectively) and the central area (CAL and CAW, respectively) were measured and the number of distal shield elements (NE) was counted (Fig. 2.1) using ImageJ 1.38 (http://rsb.info.nih.gov/ij/) at a resolution of 0.008 μm. Measurements were calibrated using 2 μm microsphere standards (Duke Scientific). The mean values of each morphological variable were calculated for each treatment.

2.3.2 Statistical analysis

Least squares linear regressions of each morphological variable as a function of salinity were calculated from data collected at 15°C, and slopes were tested against the null hypothesis that they were not significantly different from zero (*t*-test, $\alpha = 0.05$; Zar 1999). Data collected at 10, 17, and 20°C were tested against the predicted value from the 15°C regression equation to determine if temperature had a significant effect on coccolith morphology (*t*-test, $\alpha = 0.01$ after Bonferroni correction; (Sokal and Rohlf 1995; Zar 1999)).

2.3.3 Literature analysis

Coccolith distal shield and central area length and width data from sediment core-top and plankton samples with salinities between 32 and 39 (Bollmann and Herrle 2007; Bollmann et al. 2009) were used to determine the slope and intercept of each morphology – salinity relationship. The slopes and intercepts from this study were then compared to the field data (*t*-test, $\alpha = 0.05$; Zar 1999). Due to significant differences between intercepts (*see* Results), number of element data were also obtained from 22 sediment core-tops used in previous analyses (Bollmann and Herrle 2007) and compared to the culture results. A significant difference between the intercepts of the two number of element datasets prompted further analysis of the literature, which is dealt with in the Discussion. The locations of all sediment core-top, plankton, and culture samples used in this analysis are shown in Fig. 2.2 (*see* Table 2.2 for details).

2.4 Results

2.4.1 Culture coccolith morphology vs. salinity relationships

The length and width of both the coccolith distal shield and central area and the number of distal shield elements of *E. huxleyi* grown in culture were significantly related to salinity in a positive linear fashion (Table 2.1). The variable best related to salinity was distal shield length (Fig. 2.3A), although distal shield width and central area length and width all gave high r^2 values compared to the number of elements (Table 2.1). Coccoliths grown at 10, 15, 17, and 20°C were not significantly different in size.

Coccolith distal shield length varied within each treatment by a standard deviation of ~0.4 μm. However, for the purposes of determining the salinity – morphology response the linear regression through mean coccolith distal shield lengths for each salinity treatment yielded a standard error of <0.01 μm.

2.4.2 Culture comparison with plankton and sediment core-top data

There were no significant differences between the slopes of the salinity vs. morphology relationships derived from plankton and sediment core-top samples and those derived from laboratory measurements made in this study (Fig. 2.3B; Table 2.1). However, the intercepts of the culture data were significantly higher than those of both plankton and sediment core-top datasets (Fig. 2.3B; Table 2.1).

2.5 Discussion

2.5.1 Culture coccolith morphology vs. salinity relationships

The linear increase of *E. huxleyi* coccolith morphological variables with increasing salinity between 26 and 41 observed in this study supports the trends observed in previous culture work. Using salinities between 14 and 34, three out of four *E. huxleyi* strains, including the strain used here, produced smaller coccoliths at lower salinities (Green et al. 1998; Paasche et al. 1996). The culture results presented here build on these studies and show that morphological variables also respond to salinity over the range encountered in the present ocean (mostly between 33 and 38). Therefore, comparisons can be made of the relationships between coccolith morphology and salinity observed in the laboratory and those observed in the field.

2.5.2 Culture comparison with plankton and sediment core-top data

Both sediment core-top and plankton analyses (Bollmann and Herrle 2007; Bollmann et al. 2009) found *E. huxleyi* coccoliths to increase in size linearly with increasing salinities from 32 to 39 (sediment core-top data outside this salinity range are discussed later). The degree of high similarity in slopes between the coccolith morphology vs. salinity regressions for culture and for plankton and sediment core-top data (Fig. 2.3B; Table 2.1) supports the hypothesis that salinity increase causes the linear change in *E. huxleyi* coccolith size observed in the ocean (Bollmann and Herrle 2007). However, the higher intercept of the morphological data presented here indicates that the absolute sizes of coccoliths at any given salinity may be larger for culture than for environmental samples (Fig. 2.3B; Table 2.1). Therefore, here it was investigated whether culture conditions or other factors might be responsible for this size difference. For this coccolith distal shield

length data from this study and from the literature (where exact locations and salinities were known) were used.

2.5.3 Environmental effects on coccolith size

First, temperature has been shown to affect coccolith size in one *E. huxleyi* strain (Watabe and Wilbur 1966). For the strain used here, however, coccolith size remained stable at different temperatures (Fig. 2.3A). Further, the temperature range used in this study (10 – 20°C) encompasses ~35% of the data used in both plankton and sediment core-top studies (1 – 30°C; (Bollmann and Herrle 2007; Bollmann et al. 2009). Second, the nutrient replete conditions used in cultures differ from those experienced in the ocean and could be hypothesised to have caused the difference in intercepts. However, *E. huxleyi* coccolith size from other cultures grown in nutrient replete media (Table 2.2) correspond with both sediment core-top and plankton data and culture data from this study (Fig. 2.3C). Finally, the low light levels and growth rates (*see* Methods) experienced by cells in this study could also be hypothesised to have affected coccolith size. However, corresponding with the results in this study are coccolith size data (Green et al. 1998) from the same strain as is used here that were cultured at high light intensities (200 μmol photons m^{-2} s^{-1}) and experienced higher growth rates (1.0 and 1.6 d^{-1}; (Paasche et al. 1996)). Further, the growth rates experienced in this study were not linearly related to coccolith size (*see* Appendix 2.1B). Therefore, differences in temperature, nutrient and light levels, and growth rate do not appear to provide reasonable explanations of the observed size discrepancy.

While in this study salinity appears to be the main factor related to coccolith size increase, it should be noted that carbonate system components co-vary with salinity (*see* Appendix 2.2). As coccolith calcification is implicit in the carbonate system it might

reasonably be hypothesised that changes in the carbonate system might affect coccolith size. In this study a positive relationship between coccolith size and total dissolved inorganic carbon (DIC) is implied. Indeed, previous work has shown that an increase in DIC through CO_2-bubbling can result in larger coccolith sizes (Iglesias-Rodriguez et al. 2008). Therefore, the effect of DIC should be viewed as a potential mechanism for controlling coccolith size.

2.5.4 Biogeographic effects on coccolith size

Previous work suggests that coccoliths from Norwegian coastal waters belong to a larger morphotype than those in other regions (Batvik et al. 1997). Indeed, the strain used in this study (PLY B92/11) was isolated off the western coast of Norway in 1992. Further, data collected in 1991 at the start of mesocosm experiments (Batvik et al. 1997) from the same location (as the PLY B92/11 isolation site) correspond well with the culture data presented here when analysed as a function of their in situ salinity (Fig. 2.3C). Finally, data from cultured strains of *E. huxleyi* and sediment core-top samples (not corresponding with the linear salinity vs. morphology relationship) from the Oslofjord and the Skagerrak (Table 2.2) correspond well with other data from Norwegian coastal waters (Fig. 2.3D). Therefore, environmental data support the high intercept of the new culture results presented here. This provides strong evidence in favour of the suggestion (Batvik et al. 1997; Young 1994) that *E. huxleyi* populations from south-west Norwegian coastal waters belong to a local subtype (Fig. 2.3D).

Previously there has been assumed to have been a difference in *E. huxleyi* coccolith sizes between the two morphotypes A and B (Van Bleijswijk et al. 1994); type B being bigger than type A. However, the larger coccoliths from Norwegian coastal waters observed in this study belong to morphotype A (Batvik et al. 1997; Paasche et al. 1996).

Coccolith sizes from sediment core-top samples in two further geographic regions – the northern Red Sea, and the Black Sea – appear to deviate from the open ocean plankton and sediment core-top data (Fig. 2.3D). This may also indicate separate morphotypes in these marginal environments, although these data are still sparse. Nevertheless, these data, combined with those from Norwegian coastal water, suggest that *E. huxleyi* in marginal environments are morphologically different to those in the open ocean (Fig. 2.3D). The existence of genetic divides between populations from marginal waters and from the open ocean has been noted on the grounds of physiological and biochemical evidence (Conte et al. 1995; Paasche 2002). This recognition of biogeographic constraints on *E. huxleyi* morphotypes is an important step in the development of the original palaeo-SSS transfer function (Bollmann and Herrle 2007). The proxy proposed by Bollmann and Herrle (2007) is potentially still applicable to the open ocean where its calibration dataset displayed a linear salinity vs. coccolith morphology response. However, this study has shown that the original proxy is not universally applicable. Analyses of *E. huxleyi* strains from both marginal and open ocean settings are now required to ascertain the generality of the morphological divide.

2.5.5 Conclusions

In conclusion, the culture data presented in this study support a direct relationship between *E. huxleyi* coccolith morphology and salinity. This is consistent with observations from sediment core-top and plankton samples and reaffirms the potential of *E. huxleyi* coccolith morphology as a palaeo-SSS proxy. However, coccoliths from Norwegian coastal waters, the Black Sea, and the Northern Red Sea, deviate from the linear response observed in the open ocean, likely indicating different morphotypes in non-open ocean settings. It is, therefore, recommended that the coccolith morphology palaeo-SSS proxy

proposed by Bollmann and Herrle (2007) requires further evaluation before its routine application.

Table 2.1. r^2, (a) intercept, and (b) slope for linear regressions of *E. huxleyi* coccolith morphological variables (distal shield length (DL), distal shield width (DW), central area length (CAL), central area width (CAW), and number of elements (NE)) for this culture study, plankton samples (Bollmann et al. 2009), and sediment core-top samples between salinities of 33 and 39 (Bollmann and Herrle 2007). *t*-test *P* values are shown where **bold** values denote a significant difference ($\alpha = 0.05$) for comparisons of both intercept and slope of plankton and sediment core-top datasets with those of this culture study.

	Culture			Plankton					Sediment				
	r^2	a	b	r^2	a	b	*P* (a)	*P* (b)	r^2	a	b	*P* (a)	*P* (b)
DL	0.95	*1.39*	*0.07*	0.65	*-0.84*	*0.11*	**5.436**	0.414	0.67	*0.86*	*0.07*	**5.411**	0.409
DW	0.94	*0.98*	*0.06*	0.48	*0.05*	*0.07*	**5.643**	0.335	0.69	*0.41*	*0.06*	**5.527**	0.332
CAL	0.87	*0.90*	*0.03*	0.81	*-3.05*	*0.13*	**5.012**	0.285	0.20	*0.46*	*0.02*	**5.430**	0.347
CAW	0.93	*0.30*	*0.03*	0.74	*-2.30*	*0.09*	**4.973**	0.218	0.04	*0.45*	*0.01*	**5.392**	0.280
NE	0.75	*26.3*	*0.35*	-	-	-	-	-	0.47	*8.98*	*0.61*	**2.858**	1.477

Table 2.2. Data from culture, mesocosm, plankton, and sediment core-top samples used in literature analysis of coccolith distal shield length (*see* Figs. 2.2, 2.3). Location of sample or culture isolation site, and depth of sea floor are given. Data are categorised as M (marginal) or O (open ocean). No.S: number of samples or treatments. No.C: number of coccoliths per sample or treatment. Also noted is whether studies state a calibration step for SEM morphometric measurements. † Only from the initial samples for each mesocosm experiment. * Only within the range 33 – 38. ‡ Except for one datum from southern Red Sea.

Sample type	Location	Strain	Lat.	Long.	Depth (m)	M or O	No.S	No.C	Calibrated	Reference
Culture	W. Norway	B92/11	60.27	5.14	<100	M	3	av.30	Y	(Green et al. 1998)
Culture	Oslofjord	OF8	59.80	10.55	<200	M	1	60	N	(Paasche et al. 1996)
Culture	Skagerrak	SC91	58.00	9.00	<500	M	3	120	N	(Paasche et al. 1996)
Culture	W. Norway	B92/11	60.27	5.14	<100	M	13	30	Y	this study
Culture	Tasman Sea	AC472	-42.00	169.00	1000	O	1	817	N	(Beaufort et al. 2007)
Culture	Subtrop. Atlantic	DWN53/74/6	23.95	-19.52	3500	O	3	av.31	Y	(Green et al. 1998)
Culture	N. Atlantic	G1779Ga	60.00	-20.00	2500	O	2	31	Y	(Green et al. 1998)
Mesocosm	W. Norway	-	60.27	5.14	<100	M	3†	av.31	Y	(Batvik et al. 1997)
Plankton	Global	-	-	-	>1000	O	28	av.52	Y	(Bollmann et al. 2009)
Sediment	Black Sea	-	43.00	30.00	1900	M	2	50	Y	(Bollmann and Herrle 2007)
Sediment	Oslofjord	-	59.80	10.62	<200	M	2	av.51	Y	(Bollmann and Herrle 2007)
Sediment	N. Red Sea	-	-	-	<1200	M	2	av.100	Y	(Bollmann and Herrle 2007)
Sediment	Global*	-	-	-	>500	O‡	26	av.57	Y	(Bollmann and Herrle 2007)

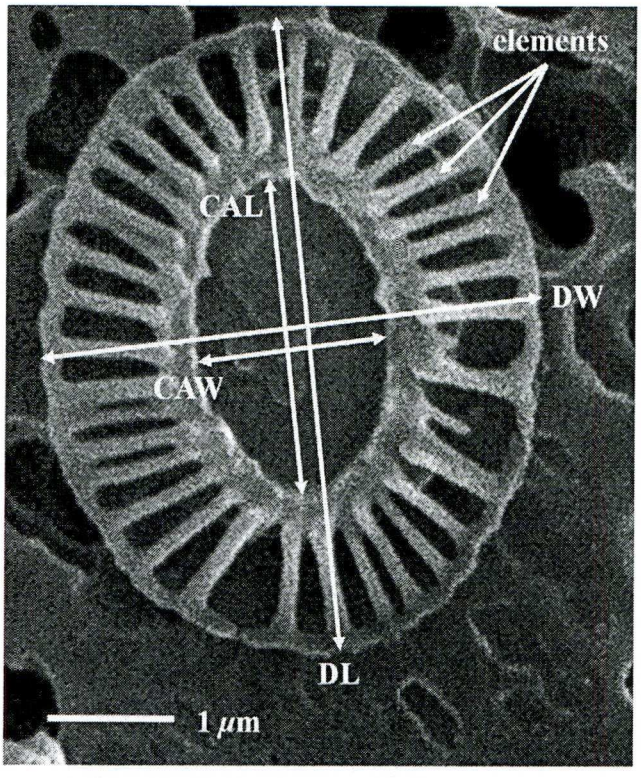

Fig. 2.1. Coccolith of *Emiliania huxleyi*, showing distal shield length (DL) and width (DW), central area length (CAL) and width (CAW), and distal shield elements.

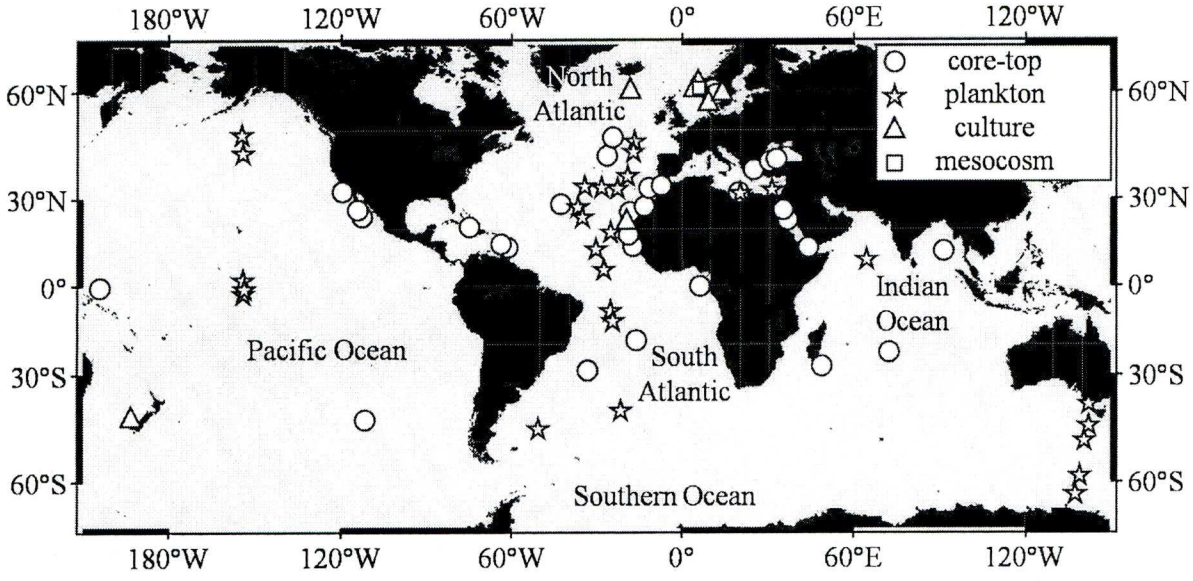

Fig. 2.2. Locations of sediment core-top (circles; (Bollmann and Herrle 2007)), plankton (stars; (Bollmann et al. 2009)), culture (triangles; this study; (Beaufort et al. 2007; Green et al. 1998; Paasche et al. 1996)), and mesocosm (squares; (Batvik et al. 1997)) samples. *See* Table 2.2 for details.

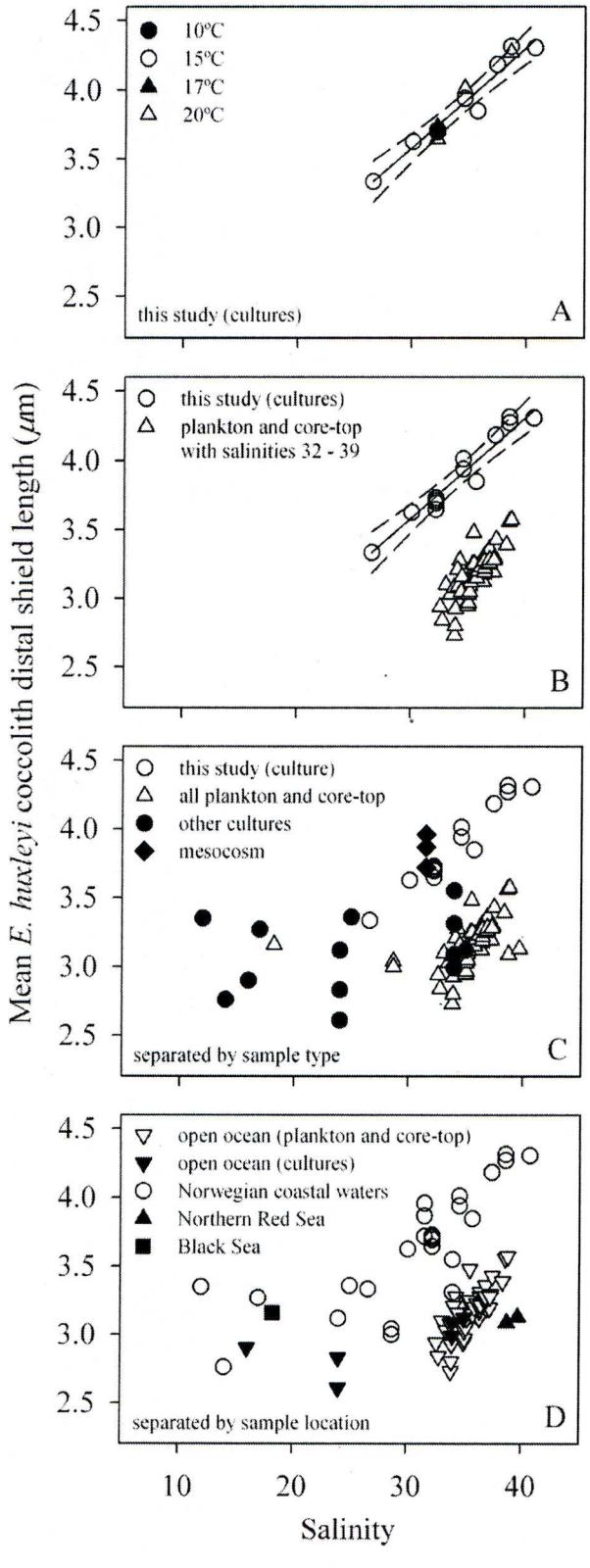

Fig. 2.3. See next page for caption

Fig. 2.3. *E. huxleyi* coccolith distal shield length measurements from this study and from the literature as a function of salinity. Solid lines represent linear regressions, dotted lines represent the 95% confidence interval. (A) Culture results from this study grown at 10°C (filled circles), 15°C (open circles), 17°C (filled triangles), and 20°C (open triangles). Linear regression is only through data from 15°C experiments. Standard deviation for each data point is ~0.4 μm. (B) Culture results from this study (open circles) and data from plankton and sediment core-top samples between salinities of 32 and 39 (open triangles; (Bollmann and Herrle 2007; Bollmann et al. 2009)). Linear regression is through data for all temperatures. (C) All literature data separated by sample type: culture results from this study (open circles), data from plankton and sediment core-top samples between salinities of 18 and 40 (open triangles; (Bollmann and Herrle 2007; Bollmann et al. 2009)), other nutrient replete cultures (filled circles; (Beaufort et al. 2007; Green et al. 1998; Paasche et al. 1996)), and data from the start of mesocosm experiments off the coast of western Norway (filled diamonds; (Batvik et al. 1997)). (D) All literature data separated by sample location: plankton and sediment core-top samples from open ocean environments (open inverted triangles), cultures from open ocean environments (filled inverted triangles), all data from Norwegian coastal waters (open circles), and sediment core-top samples from the northern Red Sea (filled triangles) and the Black Sea (filled squares). *See* Table 2.1 for more information about sample locations.

Appendix 2.1. (A) Example growth rate calculation curve showing the exponential increase in cells over time during exponential growth phase. (B) Relationship between salinity and specific growth rate for strain PLY B92/11 used in this study.

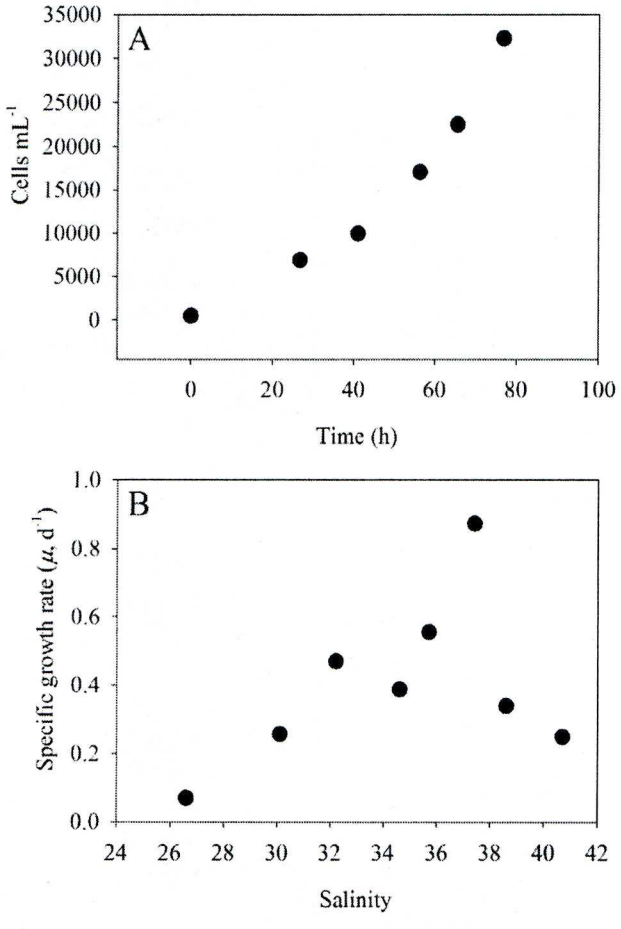

Appendix 2.2. Carbonate chemistry of seawater of varying salinities and at 15°C and 360 ppm atmospheric pCO_2. The relationship between salinity and total alkalinity (A_T) was

taken from Lee et al. (2006). Other carbonate system parameters include dissolved inorganic carbon (DIC), aqueous CO_2 (CO_{2aq}), bicarbonate ion (HCO_3^-), carbonate ion (CO_3^{2-}), and pH. Parameters were calculated using `co2sys` (http://cdiac.ornl.gov/oceans/co2rprt.html).

S	A_T (μmol kg^{-1})	DIC (μmol kg^{-1})	CO_{2aq} (μmol kg^{-1})	HCO_3^- (μmol kg^{-1})	CO_3^{2-} (μmol kg^{-1})	pH
20	1513.95	1430.76	14.61	1349.83	66.31	7.97
22	1621.89	1521.89	14.45	1430.07	77.37	7.99
24	1729.83	1611.72	14.29	1508.13	89.30	8.01
26	1837.77	1700.21	14.13	1583.92	102.15	8.02
28	1945.71	1787.31	13.97	1657.34	116.00	8.04
30	2053.65	1872.99	13.82	1728.25	130.91	8.05
32	2161.59	1957.17	13.66	1796.51	146.99	8.07
34	2269.53	2039.78	13.51	1861.94	164.33	8.08
36	2377.47	2120.76	13.36	1924.35	183.05	8.09
38	2485.41	2200.01	13.21	1983.52	203.27	8.10
40	2593.35	2277.44	13.07	2039.23	225.14	8.11
42	2701.29	2352.95	12.92	2091.23	248.80	8.12

3 Revised parameter estimates of *Emiliania huxleyi* volume to surface area ratio for alkenone-based reconstructions of atmospheric pCO_2

3.1 Abstract

The applicability of cell size-correction of the alkenone isotope palaeo-sea-surface-CO_2 proxy was assessed. Literature culture experiment data (n = 266) were collated to provide an improved parameter estimate for *Emiliania huxleyi* cell size. This updated estimate was then applied to previous palaeo-CO_2 reconstructions. The mean and range of *E. huxleyi* cell size were significantly different to those previously used, although this difference was not due to environmental variables or biogeographic differences between strains. Updated records of sea-surface-CO_2 follow the same general pattern as those made previously. However, inclusion of the updated cell size parameters approximately equate to a doubling of the error associated with reconstructing sea-surface-CO_2. Conversion of sea-surface-CO_2 records to atmospheric pCO_2 still broadly agrees with records derived from stomatal indices and boron isotopes. It is recommended that the revised *E. huxleyi* cell size estimates should be incorporated in future attempts to reconstruct sea-surface-CO_2 using alkenone isotopic ratios.

3.2 Introduction

Accurately reconstructing past variation in the partial pressure of CO_2 (pCO_2) in the atmosphere is essential to understanding how it has interacted with climate. One approach to atmospheric pCO_2 reconstruction is to first reconstruct the CO_2 concentration in past ocean surface waters ($[CO_{2(aq)}]$), which can then be converted to pCO_2. This technique uses sedimentary records of the carbon isotope fractionation of alkenone molecules that were originally produced by surface water-dwelling haptophyte algae (Jasper and Hayes 1990). Alkenone carbon isotope fractionation has a known relationship with $[CO_{2(aq)}]$ (Pagani et al. 2005), and can therefore be used for reconstruction. However, it has been shown that algal cell geometry (namely the volume to surface area ratio; V:SA) also affects carbon isotope fractionation (Popp et al. 1998b). Subsequently, records of $[CO_{2(aq)}]$ derived from alkenone carbon isotopes have been adjusted by using the V:SA of fossil haptophyte algae (Henderiks and Pagani 2007; 2008). This adjustment is made by dividing fossil haptophyte cell V:SA by the V:SA of cells of the modern haptophyte alga *Emiliania huxleyi*, which is the main source of alkenones in the present ocean together with *Gephyrocapsa* (Marlowe et al. 1990). The V:SA of *E. huxleyi* is taken to be 0.9±0.1 μm, based on a small number of measurements from a single study (Popp et al. 1998b). However, the small sample size and restricted geographical distribution of this estimate lacks statistical power. Moreover, there is strong evidence for substantial variation in *E. huxleyi* geometry (Bollmann and Herrle 2007; Bollmann et al. 2009; Fielding et al. 2009; Paasche 2002). Therefore, as *E. huxleyi* cell geometry is frequently reported in the literature, it is timely to reassess the estimates of *E. huxleyi* V:SA currently used for palaeo-atmospheric pCO_2 reconstruction.

This study aims to (1) collate all available *E. huxleyi* cell geometry data from the literature to provide a revised estimate of V:SA, (2) assess the effect of the revised V:SA estimate on the calculation of sea-surface-[$CO_{2(aq)}$] and atmospheric pCO_2, and (3) apply the revised V:SA estimate to the calculation of established records of sea-surface-[$CO_{2(aq)}$] and atmospheric pCO_2 for the Cenozoic.

3.3 Methods

All suitable *E. huxleyi* cell (excluding the coccosphere) geometry data were obtained from the literature (*see* Table 3.1). Where only organic carbon per cell was given it was converted to cell volume using the relationship given by Montagnes et al. (1994). Conversion between cell diameter, volume, and V:SA was calculated assuming spherical geometry. Data from culture material fixed in Lugol's iodine were not used as this is known to cause cell shrinkage (Montagnes et al. 1994).

Mean *E. huxleyi* V:SA was tested against the null hypothesis that it was not significantly different from the previously-used estimate of 0.9 μm (Popp et al. 1998b) using a *t*-test. The means of data from the open-ocean and from Norwegian coastal isolates were also compared. Norwegian coastal water isolates were classed as being from western Norwegian fjords, Oslofjord, and the Skagerrak; all other data were classed as open-ocean (*see* Fig. 3.1). Ordinary least squares regression was then used to determine whether culture conditions (temperature, photon flux density (PFD), and salinity) were significantly related to V:SA.

3.4 Results

Available *E. huxleyi* cell V:SA data were derived from diverse geographic locations (Fig. 3.1; Table 3.1) and from a broad range of experimental temperatures (4 – 25°C), PFDs (6 – 600 μmol photons m^{-2} s^{-1}), and salinities (30 – 36). V:SA data varied between 0.43 and 1.21 μm, and were normally distributed around a mean V:SA of 0.82 μm with a standard deviation of ~0.5 μm (Fig. 3.2).

Mean *E. huxleyi* V:SA was significantly different ($\alpha = 0.001$) to the previously-used value of 0.9 μm (Popp et al. 1998b). Further, there was no significant difference ($\alpha = 0.001$) between the means of data from the open-ocean and those from Norwegian coastal waters. However, a weak yet significant positive linear relationship was found between V:SA and PFD ($\alpha = 0.001$; $r^2 = 0.07$), although no significant relationships were found between V:SA and either temperature or salinity ($\alpha = 0.001$) (*see* Fig. 3.3).

3.5 Discussion

3.5.1 Revised V:SA estimates

The revised range of *E. huxleyi* V:SA presented here provides improved parameter estimates for the reconstruction of sea-surface-[$CO_{2(aq)}$], and thus for calculating past atmospheric pCO_2. Previously the V:SA of *E. huxleyi*, used to reconstruct upper and lower confidence intervals for past sea-surface-[$CO_{2(aq)}$], was assumed to be 0.9±0.1 μm based on a small number of measurements from two culture isolates (Popp et al. 1998b). However, by using a large sample size (n=266) of isolates from widely dispersed biogeographic provinces and a broad range of culture conditions (Fig. 3.1; Table 3.1), the dataset presented here greatly improves the accuracy and applicability of these estimates.

Nevertheless, the conversion of a proportion of the dataset from measurements of organic carbon per cell into cell size (*see* Methods) is likely to introduce additional error into the revised estimates of V:SA presented here. However, data derived from organic carbon measurements only comprise <30% of the total dataset.

The mean and range of *E. huxleyi* V:SA measured here (0.82±0.39 μm) are significantly different to those previously used to reconstruct palaeo-pCO_2 (Henderiks and Pagani 2007; 2008). However, the revised dataset is derived from a broader spectrum of biogeographic locations and environmental conditions, and this may affect V:SA. Therefore, the dependence of V:SA on these factors is discussed.

3.5.2 Environmental and biogeographic effects on V:SA

Previously, both environmental conditions and the biogeographic provenance of *E. huxleyi* isolates and samples were seen to impact their morphometry (Bollmann and Herrle 2007; Bollmann et al. 2009; Fielding et al. 2009; Paasche 2002). Therefore, the V:SA data presented in this study are potentially biased by these factors.

First, isolates and samples of *E. huxleyi* from Norwegian coastal waters have larger coccoliths than their open-ocean counterparts (Fielding et al. 2009). As coccolith size is often assumed to be proportional to cell size (and therefore V:SA), the inclusion of Norwegian coastal isolates in the dataset presented here may skew the mean and maximum V:SA towards higher values. However, there is no significant difference between the means of Norwegian coastal water and open-ocean isolates. Further, the maximum V:SA of Norwegian coastal water data was lower than that of open-ocean *E. huxleyi* isolates. Therefore, the difference between these two biogeographically restricted groups observed for coccolith morphology does not appear to hold true for cell morphology.

Second, salinity is linearly related to coccolith sizes across the range observed in this study (30 – 36) (Bollmann and Herrle 2007; Bollmann et al. 2009; Fielding et al. 2009). Again, assuming coccolith size is proportional to cell size and therefore V:SA, salinity would be expected to have an effect on the V:SA data in this study. Salinity values are only available for approximately half of the dataset (n=130), although where it was not reported it is unlikely to have been far outside 30 – 36. Nevertheless, for the subset of the data where it is available, salinity cannot explain variation in V:SA suggesting that cell size is not directly related to coccolith size.

Finally, low PFD can cause a reduction in *E. huxleyi* cell V:SA, while phosphorus limitation can cause *E. huxleyi* V:SA to increase (Paasche 2002). Further, temperature is often negatively correlated with cell size for a wide variety of protists (Atkinson et al. 2003). Only 5% of the data presented here are from phosphorus-limited culture, and as such are unlikely to bias results. However, the data are derived from a large range of PFDs and temperatures (*see* Results). While, temperature is not significantly related to V:SA, the weak relationship between PFD and V:SA may explain some of the observed variation in this dataset. However, data are evenly distributed across the range of PFDs. Therefore, even though low light may skew V:SA toward lower values, the distribution of the data across the environmental range means that this is unlikely to significantly bias results.

3.5.3 Potential implications for CO_2 reconstruction

The revised *E. huxleyi* V:SA estimates are clearly different from those made previously. However, it is pertinent to quantify the impact of this difference on alkenone-based reconstructions of past sea-surface-$[CO_{2(aq)}]$ (e.g. Henderiks and Pagani 2008). Figure 3.4 highlights the impact of using revised compared to original *E. huxleyi* V:SA estimates across the ranges of alkenone carbon isotope fractionation and fossil cell V:SA

that are found in the sedimentary record (Henderiks and Pagani 2008). This analysis shows that the difference between original and revised sea-surface-[$CO_{2(aq)}$] increases towards higher values of fossil V:SA and alkenone carbon isotope fractionation. However, both fossil V:SA and alkenone carbon isotope fractionation vary independently in the sedimentary record (Henderiks and Pagani 2008), and therefore, the impact of the revised estimates of *E. huxleyi* V:SA on these data is quantified.

3.5.4 Revised alkenone-based Cenozoic CO_2 reconstruction

The longest available record of sedimentary alkenone carbon isotope fractionation and cell V:SA over the Cenozoic (Henderiks and Pagani 2008) is used here to assess the implications of the revised *E. huxleyi* V:SA estimates. The mean and upper and lower confidence interval for Cenozoic sea-surface-[$CO_{2(aq)}$] can be calculated in the same way as Henderiks and Pagani (2008) using the mean and 95% confidence intervals for both previously-used (Popp et al. 1998b) and revised *E. huxleyi* V:SA to give original and revised estimates for [$CO_{2(aq)}$]. There is no difference in the general trend of both original and revised [$CO_{2(aq)}$] reconstructions (Fig. 3.5), although the original *E. huxleyi* V:SA underestimates mean [$CO_{2(aq)}$] throughout the time period examined (Fig. 3.5). Revised mean [$CO_{2(aq)}$] is ~1 μmol kg^{-1} higher in the Miocene and up to ~3 μmol kg^{-1} higher in the Eocene. Further, confidence intervals for revised [$CO_{2(aq)}$] are larger than those for original [$CO_{2(aq)}$]. Confidence intervals are still small for revised Miocene estimates but are ~6 μmol kg^{-1} wider than those estimated using the original *E. huxleyi* V:SA. This difference is more noticeable in the Eocene where revised confidence intervals for [$CO_{2(aq)}$] are ~30 μmol kg^{-1} larger than the original (Henderiks and Pagani 2007) (Fig. 3.5). Notably, throughout the time interval studied, error estimates for [$CO_{2(aq)}$] were consistently around double those made previously.

These differences in $[CO_{2(aq)}]$ can be converted to equivalent atmospheric pCO_2 using the solubility coefficient for CO_2 (Weiss 1974), and assuming equilibrium between seawater and the atmosphere. The solubility coefficient is dependent on temperature and to a lesser extent on salinity. Therefore, previous conversions from $[CO_{2(aq)}]$ to pCO_2 were adjusted (Henderiks and Pagani 2008) using palaeo-sea-surface temperature records derived from oxygen isotopes (Zachos et al. 2001). However, oxygen isotope-derived temperatures are affected by global ice volume and changes in varying latitudinal evaporation and precipitation. Therefore, as the Cenozoic record spans the onset of Antarctic glaciation (~33 Myr ago), their application to this dataset is not straightforward. Therefore, as the Cenozoic data are from temperate open-ocean sites (Henderiks and Pagani 2008), the conversion between $[CO_{2(aq)}]$ and pCO_2 made here assumes a temperature of 18°C and a salinity of 35. Conversion of sea-surface-$[CO_{2(aq)}]$ to atmospheric pCO_2 in this fashion yields an upper confidence interval for pCO_2 of up to ~500 p.p.m. (Miocene), ~3100 p.p.m. (Eocene-Oligocene boundary), and ~2100 p.p.m. (Eocene), while mean revised pCO_2 is on average ~100 p.p.m. higher than the original (Fig. 3.5). However, these values should be interpreted with caution as sea-surface temperatures and salinities are unlikely to have been constant through time (e.g. Hay et al. 2006). Nevertheless, the revised *E. huxleyi* V:SA presented in this study introduces added but realistic uncertainty into estimates of palaeo-atmospheric pCO_2.

3.5.5 Cenozoic atmospheric pCO_2 records

Estimates of atmospheric pCO_2 derived using other techniques (Demicco et al. 2003; Pearson et al. 2009; Royer 2006) are available for the time periods immediately before and after that of the data analysed in this study (16 – 45 Myr ago), with some overlapping data in the late Eocene (Fig. 3.6). The revised pCO_2 record estimated here

broadly agrees with these other datasets. Revised upper and lower confidence intervals correspond well with the adjacent stomatal and boron isotope-derived estimates in the middle Miocene, and with those from boron isotope-derived, but not stomatal, pCO_2 concentrations at the Eocene-Oligocene boundary. However, the upper confidence interval of ~2000 p.p.m. at around 45 Myr ago is at odds with the upper estimates of ~700 p.p.m. calculated using stomatal and boron isotopic techniques (Fig. 3.6). It has previously been highlighted that the alkenone-based pCO_2 proxy loses precision at high values of carbon isotope fractionation (Royer et al. 2001) such as those observed here in the Eocene; and the inclusion of upper and lower confidence intervals for *E. huxleyi* V:SA exacerbates this lack of precision.

3.5.6 Conclusions

The data presented here provide improved parameter estimates of the volume to surface area ratio of *E. huxleyi*, which have been used to reconstruct past atmospheric pCO_2. These revised estimates do not alter the general trend of pCO_2 previously observed over the Cenozoic (Henderiks and Pagani 2008). However, the revised parameter estimates greatly decrease the precision of such reconstructions compared to the range of *E. huxleyi* V:SA used previously. This is especially evident for the higher pCO_2 in the Oligocene and Eocene. Nevertheless, it is recommended that the revised *E. huxleyi* V:SA estimates presented here are used for future pCO_2 reconstructions, due to their greater statistical power compared to previous estimates.

Table 3.1. *E. huxleyi* isolates used to compile revised estimates of cell V:SA in this study. The latitude and longitude, number of V:SA measurements, and range of V:SA is given for each isolate.

Isolate	Lat.	Lon.	*n*	V:SA (μm)	Reference
88E	43	-68	4	0.89 - 1.11	(Fernandez et al. 1996a)
Bergen	60	5	4	0.85	(Ramos et al. 2010)
CCMP#1516	-3	-83	1	0.86	(Steinke et al. 1998)
CCMP#370	60	11	1	0.73	(Steinke et al. 1998)
CCMP#371	32	-62	8	0.81 - 0.93	(Feng et al. 2008)
CCMP#373	32	-65	4	0.68 - 0.88	(Shaw et al. 2003; Steinke et al. 1998; Sunda and Hardison 2007)
CCMP#374	43	-69	7	0.76 - 0.83	(Bucciarelli et al. 2007; Steinke et al. 1998; Sunda et al. 2007)
CCMP#378	43	-68	8	0.68 - 1.21	(Keller et al. 1999a; Keller et al. 1999b)
CCMP#379	50	-4	1	0.80	(Steinke et al. 1998)
Ch24-90	57	1	3	0.43 - 0.68	(Van Bleijswijk et al. 1994)
Ch25-90	57	1	3	0.45 - 0.71	(Van Bleijswijk et al. 1994)
EH2	-19	148	4	0.69 - 0.83	(Sorrosa et al. 2005)
L	60	11	61	0.61 - 1.05	(Buma et al. 2000; Riegman et al. 2000; Steinke et al. 1998; Van Rijssel and Buma 2002; Van Rijssel and Gieskes 2002)
MS1	48	-17	1	0.58	(Stoll et al. 2002a)
NAP9	41	14	4	0.70 - 0.77	(Paasche 1999)
NEPCC#55a	50	-145	22	0.76 - 1.03	(Prahl et al. 2003)
NEPCC#732	50	-145	40	0.52 - 0.78	(Lecourt et al. 1996; Muggli and Harrison 1996a; Muggli and Harrison 1996b; Needoba and Harrison 2004; Needoba et al. 2003; Varela and Harrison 1999)
PLY#B92/11	60	5	46	0.76 - 1.08	(Riebesell et al. 2000; Rost et al. 2002)
PLY#BOF92	48	-17	20	0.65 - 1.09	(Paasche 1998; Paasche 1999)
RCC#1212	-34	17	4	0.97 - 1.02	(Langer et al. 2009a)
RCC#1216	-42	170	4	0.96 - 1.03	(Langer et al. 2009a)
RCC#1238	34	140	4	0.93 - 0.99	(Langer et al. 2009a)
RCC#1256	63	-20	4	1.02 - 1.13	(Langer et al. 2009a)
SC91	58	9	4	0.74 - 0.79	(Paasche 1999)
TW1	41	2	4	0.63	(Sciandra et al. 2003)

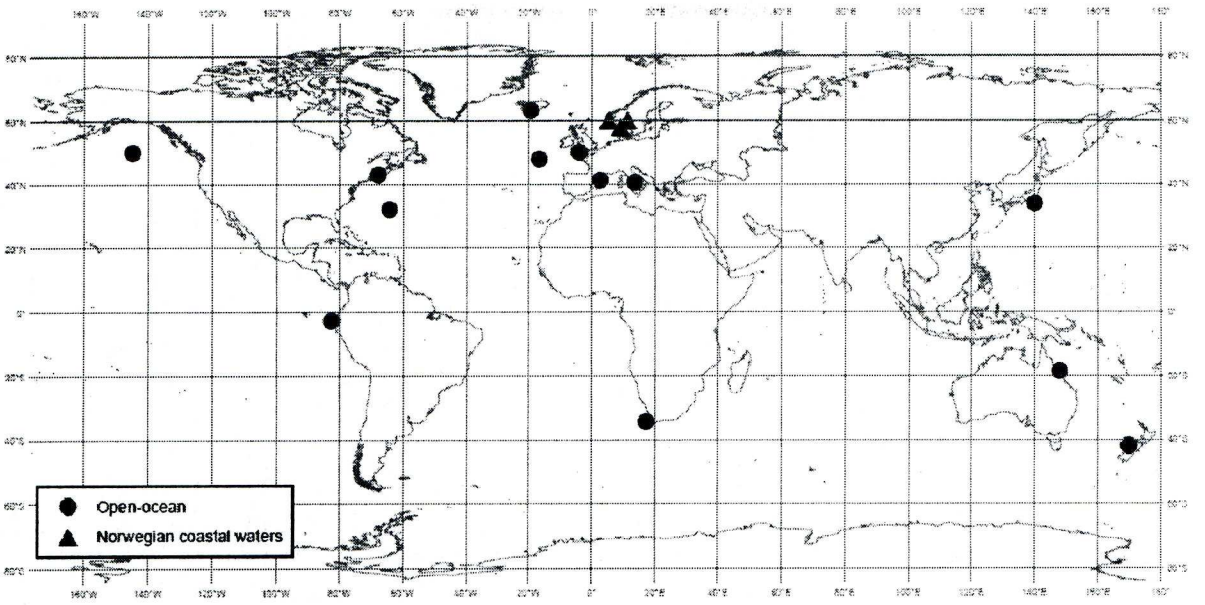

Fig. 3.1. Locations of open-ocean (circles) and Norwegian coastal water (triangles) *E. huxleyi* isolates. *See* Table 3.1 for details.

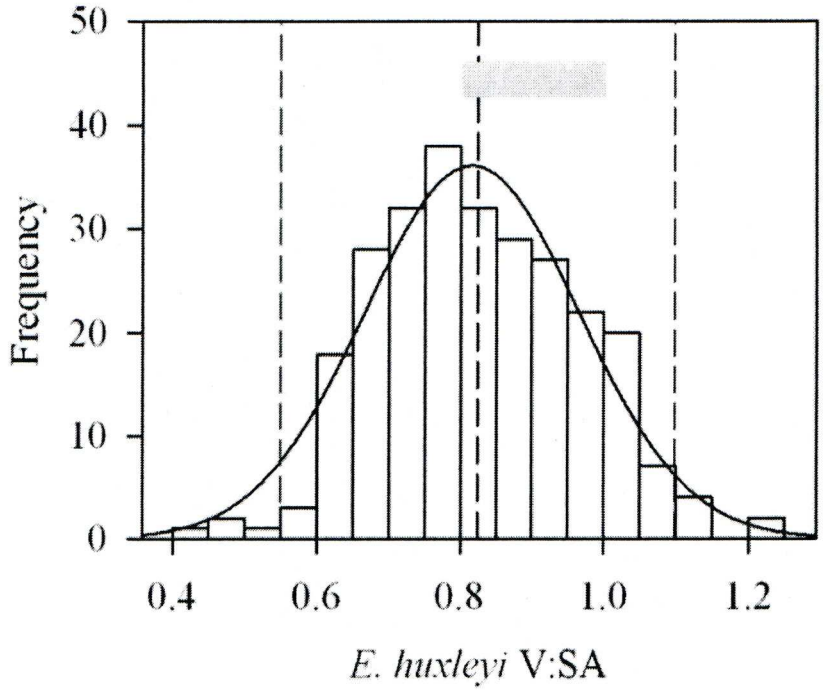

Fig. 3.2. Histogram of all *E. huxleyi* V:SA data with a normal distribution curve (solid line) around the mean, and the mean and 95% confidence intervals (dashed lines). The range of *E. huxleyi* V:SA previously used for atmospheric pCO_2 reconstruction is also shown (grey bar; *see* text).

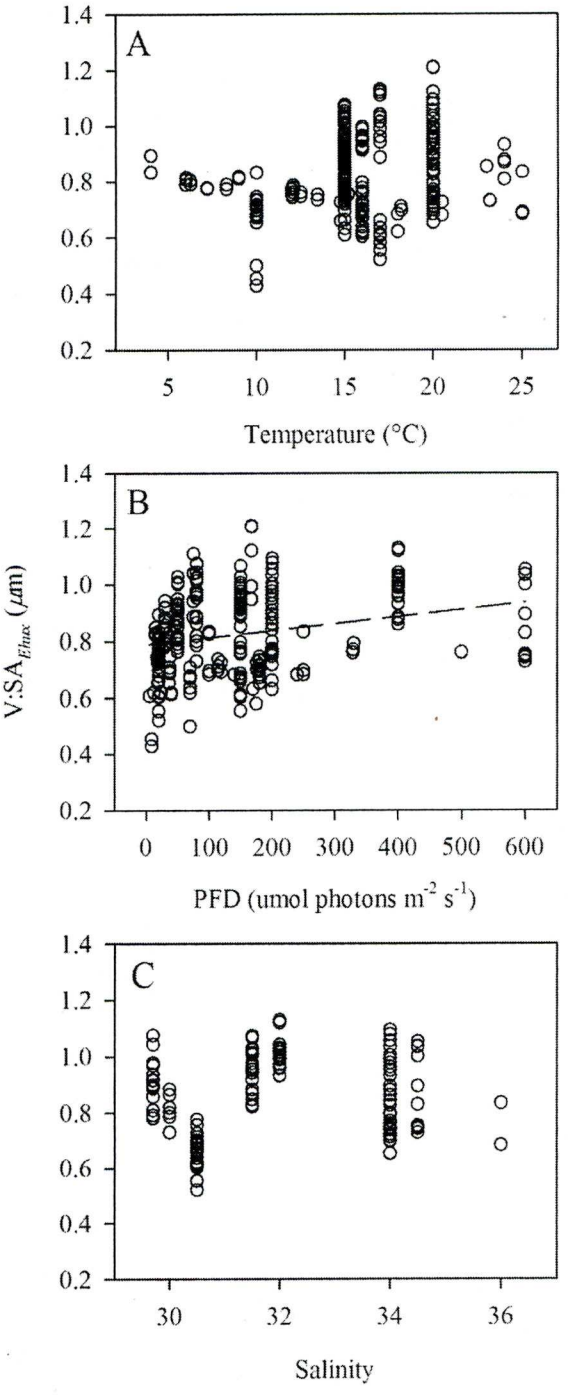

Fig. 3.2. *E. huxleyi* V:SA data as a function of (A) temperature, (B) photon flux density, and (C) salinity. The dotted line in (B) represents a linear regression (r^2 = 0.07). There were no significant relationships between either temperature or salinity and V:SA (α = 0.001).

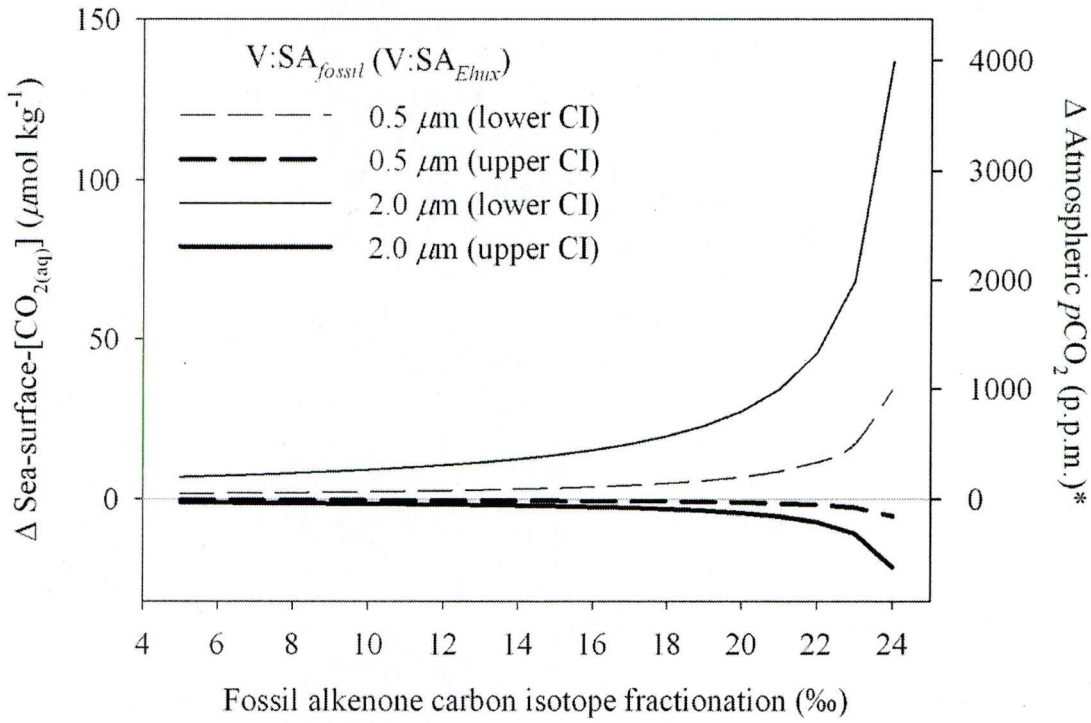

Fig. 3.4. Difference between sea-surface-[$CO_{2(aq)}$] calculated using revised and original *E. huxleyi* V:SA (*see* text) across a range of fossil alkenone carbon isotope fractionation and fossil haptophyte V:SA. Higher Δ values show that the original V:SA underestimates sea-surface-[$CO_{2(aq)}$] compared to the revised value, while lower Δ values indicate an overestimation. The calculation is made using both small (0.5 μm; dashed lines) and large (2.0 μm; solid lines) fossil V:SA, and using both the lower (thin lines) and upper (thick lines) 95% confidence intervals for *E. huxleyi* V:SA. *Equivalent atmospheric pCO_2 is shown assuming a solubility coefficient at T=18°C and S=35 (Weiss 1974).

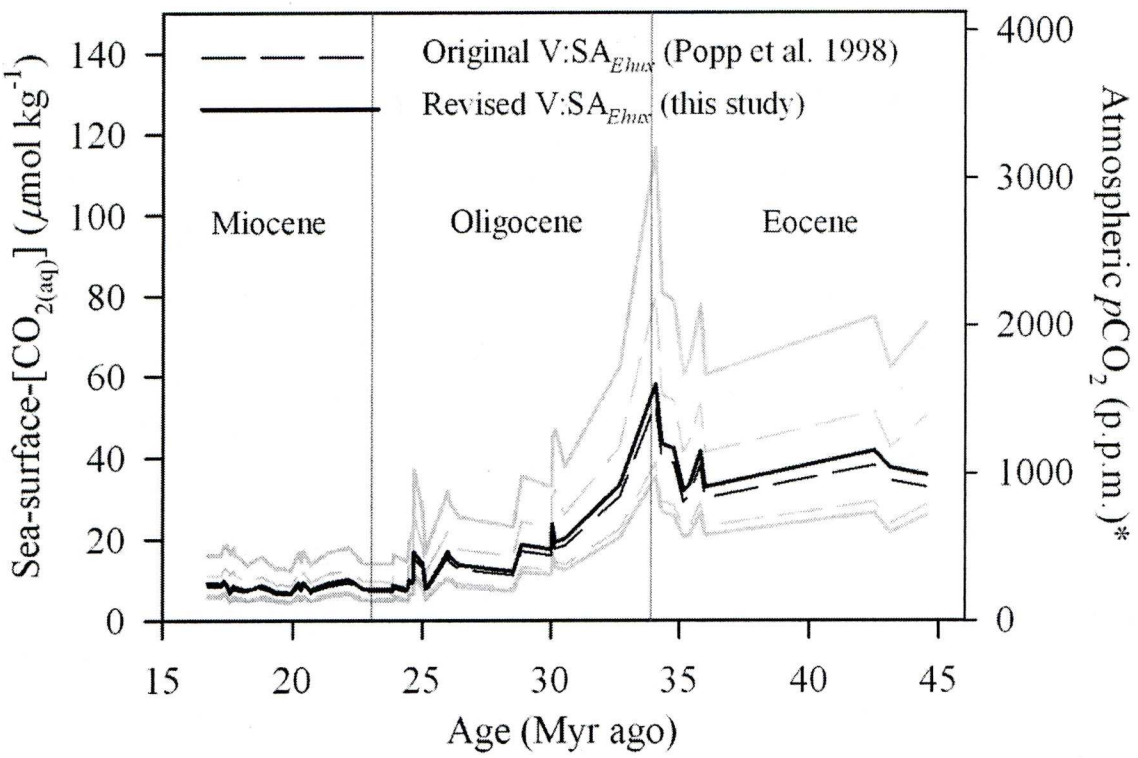

Fig. 3.5. Alkenone-derived sea-surface-[$CO_{2(aq)}$] over part of the Cenozoic. [$CO_{2(aq)}$] is calculated using fossil alkenone carbon isotope fractionation, fossil haptophyte cell V:SA, and sea-surface phosphate concentration estimates from Henderiks & Pagani (2008), together with original (Popp et al. 1998b) and revised (this study) *E. huxleyi* V:SA estimates. Mean [$CO_{2(aq)}$] is calculated using the means of both original (dashed black line) and revised (solid black line) *E. huxleyi* V:SA, together with the means of all other input variables. Lower and upper confidence intervals (grey lines) were calculated from minimum and maximum values of all input variables, and from the 95% confidence intervals of original (dashed grey lines) and revised (solid grey lines) *E. huxleyi* V:SA estimates. *Equivalent atmospheric pCO_2 is shown assuming a solubility coefficient at T=18°C and S=35 (Weiss 1974).

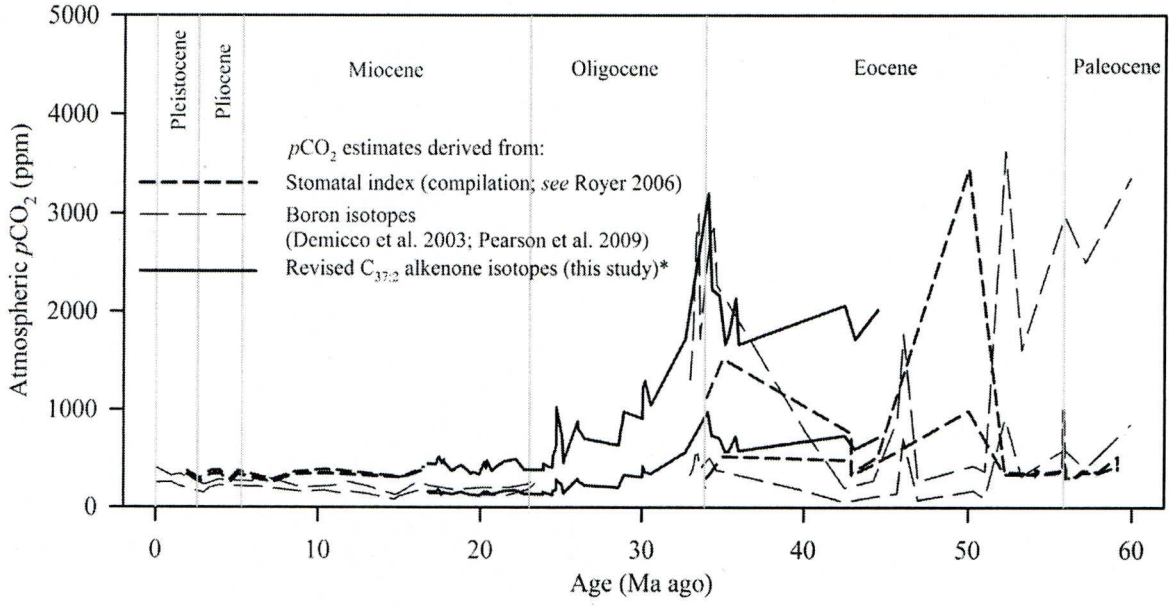

Fig. 3.6. Cenozoic atmospheric pCO_2 records from stomatal index (short dashed line; compilation in Royer 2006), boron isotope (long dashed line; Demicco et al. 2003; Pearson et al. 2009), and revised alkenone carbon isotope techniques (solid line; this study). *Atmospheric pCO_2 records from alkenone carbon isotopes are calculated assuming a solubility coefficient at T=18°C and S=35 (Weiss 1974). For potential caveats of this method *see* Discussion.

4 A potential mechanism for elevated coccolith Sr/Ca in an *Emiliania huxleyi* bloom

4.1 Abstract

The potential contribution of *Emiliania huxleyi* bloom formation to coccolith Sr/Ca is quantified using a Rayleigh distillation box model. Coccolith Sr/Ca is currently believed to be dependent on productivity and temperature. However, this study highlighted that *E. huxleyi* coccolith Sr/Ca would also increase with the quantity of coccoliths produced and with decreasing salinity. Based on measurements of the quantity of coccolith produced in a bloom scenario the maximum effect of a bloom of coccolith Sr/Ca was 0.38 mmol mol^{-1}. This figure is comparable with the variation in *E. huxleyi* Sr/Ca in the sedimentary record which can be up to 1.30 mmol mol^{-1}. Therefore, part of the variation in the sedimentary Sr/Ca record may be due to bloom occurrence in certain areas of the ocean. The findings presented here do not negate the use of coccolith Sr/Ca as a palaeoproductivity indicator. However, they serve to highlight a potential mechanism for controlling *E. huxleyi* coccolith Sr/Ca.

4.2 Introduction

The marine algal group, the coccolithophores, mediate global carbon and sulphur cycles by synthesising both inorganic carbon, and organic carbon and sulphur. Reconstructing the past productivity of coccolithophores is therefore important for understanding their contribution to fluxes of both carbon and sulphur across the air-sea boundary and from ocean surface-waters to the sediments.

Sedimentary records of the ratio of Sr to Ca (Sr/Ca) in coccoliths are positively related to past coccolithophore production (Rickaby et al. 2007). This relationship has been supported by culture experiments which suggest that coccolith Sr/Ca increases with increasing coccolithophore calcification rate, and to a lesser extent, due to increasing temperature (Rickaby et al. 2002; Stoll et al. 2002b).

However, trace element incorporation into biogenic calcite has also been demonstrated to be partly due to the effects of Rayleigh distillation acting through Ca depletion in the fluid reservoir used for calcification (Elderfield et al. 1996). Primarily, the relationship between the Sr/Ca in the calcification reservoir and the Sr/Ca of the calcite at any instance in time can be defined by the constant exchange coefficient,

$$\alpha = \frac{\mathrm{Sr/Ca_{calcite}}}{\mathrm{Sr/Ca_{fluid}}}$$

Rayleigh distillation only occurs if the calcification reservoir has a finite volume. If $\alpha < 1$, the reservoir Sr/Ca will increase as calcite precipitation preferentially removes a larger proportion of Ca than it does of Sr from the fluid reservoir. In turn, the changing reservoir Sr/Ca will act to increase calcite Sr/Ca if the exchange coefficient remains

constant. Therefore, assuming the calcification reservoir is of finite volume, calcite Sr/Ca will be increasingly altered as more calcite is precipitated.

Coccolith Sr/Ca can, therefore, be affected by coccolithophore calcification rate, the Sr/Ca of the surrounding fluid reservoir (i.e. seawater), and by the amount of calcite precipitated. As highlighted above, calcification rate has a marked effect, both in culture experiments and in the ocean. Seawater Sr/Ca has varied over time (Stoll and Schrag 1998) but only varies by a small amount in the present surface ocean (De Villiers 1999). However, the effect of the quantity of calcite precipitation on Sr/Ca has not yet been investigated.

Coccolithophore blooms present a scenario where the concentration of coccolith calcite is high at the site of its precipitation and where coccolith Sr/Ca might therefore be significantly affected by Rayleigh distillation by altering the Sr/Ca of the surrounding seawater. Further, blooms can contribute significantly to the sedimentary coccolith Sr/Ca signal in certain areas of the ocean (Bijma et al. 2001).

In this study, the effect of Rayleigh distillation on coccolith Sr/Ca is calculated for varying concentrations of calcite assuming a finite calcification reservoir, and the results are applied to a hypothetical *Emiliania huxleyi* bloom scenario. The coccolithophore *E. huxleyi* is used in the model due to its bloom-forming nature and due to there being sufficient data regarding its bloom characteristics and its Sr/Ca exchange coefficient.

4.3 Methods

The change in coccolith Sr/Ca as a function of the quantity of coccolith Ca precipitated was calculated in a similar way to the Rayleigh distillation-type box model

described by Elderfield et al. (1996). In the model used in this study, change in seawater Sr/Ca (Sr/Ca_{SW}) over time can be expressed by,

$$\frac{Sr/Ca_{SW}}{Sr/Ca^{0}_{SW}} = f^{\alpha-1}$$

where Sr/Ca^{0}_{SW} is the original seawater Sr/Ca, and f is the fraction of Ca remaining in solution. *E. huxleyi*-specific values for α were derived from the literature (Table 4.1). The coccolith Sr/Ca (Sr/Ca_{COCC}), accumulated over time following changing Sr/Ca_{SW}, was integrated using the mass balance equation:

$$Sr/Ca^{0}_{SW} = f \times Sr/Ca_{SW} + (1 - f) \times Sr/Ca_{COCC}$$

Initial values of seawater [Sr] and [Ca] (normalised to a salinity of 35) were obtained from the literature (Table 4.1). The model assumes no back-reaction between solid (calcite) and liquid (reservoir) states.

4.4 Results

4.4.1 Model parameters from the literature

At a salinity of 35, literature values of seawater [Sr] vary by 33.88 μmol kg^{-1}, while [Ca] varies by 1.18 mmol kg^{-1} (Table 4.1). Literature values for α vary from 0.13 to 0.65 (Table 4.1).

4.4.2 Model output

For all combinations of input parameters, seawater Sr/Ca and incremental and cumulative coccolith Sr/Ca generally increase as the reservoir of Ca is depleted by coccolithophore calcification (Fig. 4.1). For *E. huxleyi*, coccolith Sr/Ca increases linearly

as increasing quantities of Ca are precipitated and removed from the calcification reservoir. Figure 4.2A shows the maximum potential change in *E. huxleyi* coccolith Sr/Ca given all permutations of the input parameters (α, [Sr], and [Ca]) at a salinity of 35. Change in coccolith Sr/Ca is also increased under lowered salinity (Fig. 4.2B) due to lower initial reservoir concentrations of both Sr and Ca.

4.5 Discussion

4.5.1 Calcite production in a bloom scenario

To apply these model results to real-world *E. huxleyi* blooms, knowledge of the quantity of coccolith Ca precipitated is required. The highest recorded concentration of *E. huxleyi* cells in a bloom was 1.15×10^{8} cells L^{-1} (Berge 1962), while there can be up to ~250 coccoliths per cell in the later stages of a bloom (e.g. Balch et al. 1996b). This equates to a maximum concentration of 2.88×10^{10} coccoliths L^{-1}. Young & Ziveri (2000) provide equations for calculating the calcite content of individual coccoliths given their length; a maximum coccolith length of ~4.25 μm (Fielding et al. 2009) would give 4.14×10^{-14} mol Ca coccolith^{-1}. Using the above values the maximum Ca concentration in a bloom would be 1.10 mmol Ca L^{-1}. It should be noted however, that this is an 'extreme-case scenario', and many blooms are not likely to achieve these Ca concentrations.

However, assuming this 'extreme-case scenario', cumulative coccolith Sr/Ca would be elevated by ~0.38 mmol mol^{-1} from its pre-bloom value, whereas calcite produced at the end of the bloom (the final increment) would be elevated by ~0.78 mmol mol^{-1} from its pre-bloom value (Fig. 4.2A). Therefore, an increase in *E. huxleyi* coccolith Sr/Ca by this magnitude in the sediment record may reflect past bloom occurrence.

4.5.2 Comparison with natural coccolith Sr/Ca variation

E. huxleyi coccolith Sr/Ca in culture experiments can vary by up to ~1.10 mmol mol^{-1} (Stoll et al. 2007b). However, there have been few measurements of *E. huxleyi* coccolith Sr/Ca in the ocean. Sediment-trap data from the Sargasso Sea (not notably an *E. huxleyi* bloom area) only show a variation of ~0.10 mmol mol^{-1} (Stoll et al. 2007b). This lack of data is largely due to methodological constraints on measuring the Sr/Ca of individual coccolithophore species, and has resulted in the majority of core-top and down-core coccolith Sr/Ca records being based on bulk coccolith carbonate. Bulk (i.e. multi-species) sedimentary coccolith Sr/Ca can vary by ~0.70 mmol mol^{-1} in the Pacific, ~1.30 mmol mol^{-1} in the Atlantic, and ~0.50 mmol mol^{-1} in the Indian Ocean (Rickaby et al. 2007). However, there are notable systematic differences between the coccolith Sr/Ca of individual species (Stoll et al. 2002c) making it difficult to compare these ranges to that potentially generated by *E. huxleyi*. It should be noted however, that the largest variation in *E. huxleyi* Sr/Ca was observed in the North Atlantic (Rickaby et al. 2007) which is a major *E. huxleyi* bloom region. Therefore, it is possible that this variation is due to the effect of bloom-formation on *E. huxleyi* coccolith Sr/Ca described in this study.

4.5.3 Bloom occurrence in relation to salinity

The effect of a change in salinity from 30 to 40 on cumulative coccolith Sr/Ca in this study is relatively small, being less than 0.05 mmol mol^{-1} (Fig. 4.2B). Further, the majority of *E. huxleyi* bloom production occurs in temperate latitudes (Iglesias-Rodriguez et al. 2002) where the salinity stays within a narrow range between 32 and 35 (Antonov et al. 2006). Salinity has been lower in these regions in the past; at the Last Glacial Maximum salinity in the North Atlantic dropped by ~4 (Kim et al. 2003). However, the effect of this difference in salinity on bloom coccolith Sr/Ca is marginal compared to that

of the level of coccolith production. Bloom areas where low salinity would have more of an effect on coccolith Sr/Ca would be the Norwegian fjords where salinity is often below 30.

4.5.4 Constraints on model application

The model outlined in this study relies on the assumption that the pool of Sr and Ca in the seawater in the bloom is finite (i.e. it is a closed-box model). For a small bloom which forms slowly a closed-box model is an unlikely scenario as mixing with seawater outside the bloom would occur faster than Sr and Ca depletion. However, larger and more rapidly forming blooms may come close to replicating the closed-box model scenario discussed earlier. Unfortunately, there do not appear to be any available measurements of seawater Sr or Ca concentrations in *E. huxleyi* blooms. It has been noted that blooms most frequently occur when the water column is strongly stratified (Tyrrell and Merico 2004) thus limiting replenishment of Sr and Ca by vertical mixing. Further, blooms can cover extremely large areas of ocean, the largest being ~1×10^6 km^2 (Raitsos et al. 2006). Therefore, although blooms appear to be dispersed primarily by lateral mixing (Balch et al. 2009), seawater in the centre of such large blooms would likely be buffered to an extent against replenishment of Sr and Ca by lateral mixing.

4.5.5 Conclusion

As mentioned previously, the model output for this study represents an 'extreme-case scenario'. In both modern and past oceans the initial seawater Sr/Ca and salinity will vary and mixing will occur. The results do not alter the general conclusions of previous empirical work where elevated sedimentary coccolith Sr/Ca is assumed to be related to increased past coccolithophore bloom productivity (Rickaby et al. 2007; Stoll et al. 2007a). However, the results highlight a potential mechanism by which *E. huxleyi* coccolith Sr/Ca

might act as a tracer of bloom occurrence complementary to its ability to record coccolith calcification rate.

Table 4.1. Minimum and maximum values for model input parameters derived from the literature including seawater concentrations of Sr and Ca normalised to a salinity of 35 and the exchange coefficient for Sr between seawater and coccolith calcite (α).

Min	*Max*	Reference
Seawater $[Ca]_{N35}$ (mmol kg^{-1})		
9.67	10.78	(Billings et al. 1969)
10.19	10.35	(Culkin and Cox 1966)
10.18	10.31	(De Villiers 1998)
10.18	10.21	(De Villiers and Nelson 1999)
9.96	10.54	(Fabricand et al. 1967)
10.30	10.31	(Horibe et al. 1974)
10.23	10.29	(Krumgalz and Holzer 1980)
9.90	10.85	(Muller and De Deckker 2002)
10.35	10.48	(Naqvi and Reddy 1979)
10.83	10.85	(Sen Gupta et al. 1978)
10.18	10.32	(Tsunogai et al. 1968)
9.67	**10.85**	**All**
Seawater $[Sr]_{N35}$ (μmol kg^{-1})		
64.52	69.94	(Andersen and Hume 1968)
64.57	98.40	(Andersen et al. 1970)
85.13	86.39	(Bernat et al. 1972)
82.92	95.74	(Billings et al. 1969)
85.02	91.03	(Brass and Turekian 1972)
86.92	88.04	(Brass and Turekian 1974)
90.11	96.24	(Chow and Thompson 1955)
84.02	90.66	(Culkin and Cox 1966)
88.98	88.98	(De Villiers 1999)
87.12	91.10	(Fabricand et al. 1966)
87.56	91.32	(Fabricand et al. 1967)
91.83	93.77	(Mackenzie 1964)
86.25	91.75	(Muller and De Deckker 2002)
92.43	95.96	(Nagaya et al. 1971)
64.52	**98.40**	**All**
α		
0.32	0.65	(Langer et al. 2006)
0.30	0.39	(Langer et al. 2009b)
0.13	0.64	(Rickaby et al. 2002)
0.28	0.30	(Stoll et al. 2002a)
0.13	**0.65**	**All**

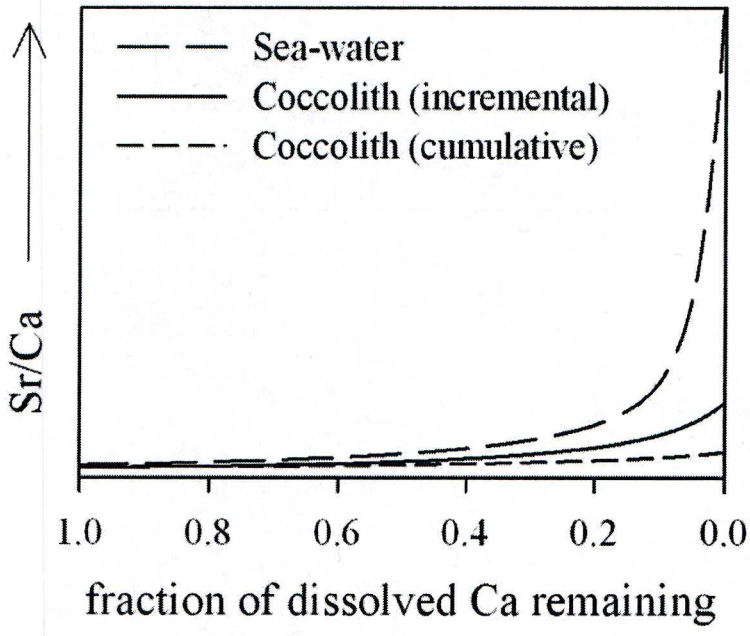

Fig. 4.1. General relationship between seawater Ca depletion and the Sr/Ca of seawater and coccolith calcite.

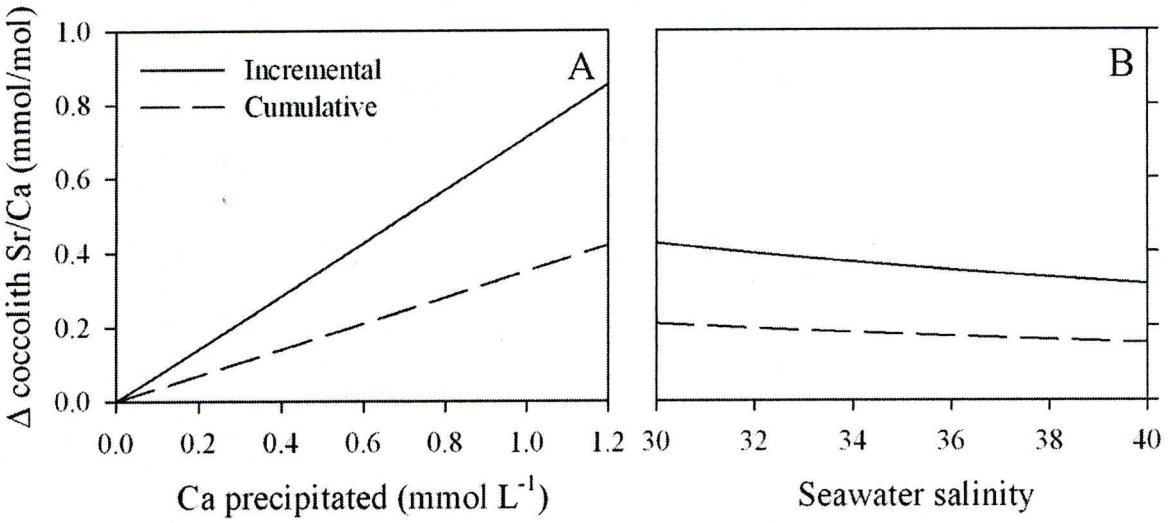

Fig. 4.2. Maximum change in incremental and cumulative *E. huxleyi* coccolith Sr/Ca as a function of Ca precipitation as coccolith calcite at a salinity of 35 (A), and as a function of seawater salinity with a removal of 0.5 mmol Ca L^{-1} (B).

5 Revised estimates of *Emiliania huxleyi* specific growth rate dependence on temperature

5.1 Abstract

A revised estimate of the relationship between *E. huxleyi* growth rate and temperature was made using literature data from culture experiments (n = 1051) combined with quantile regression. For modelling *E. huxleyi* bloom formation, this relationship is commonly assumed to follow an exponential relationship, as is the case for photosynthetic algal species in general. However, the results in this study demonstrate that, for data specific to *E. huxleyi*, this relationship is better described by a power function. It is recommended that the revised relationship between *E. huxleyi* growth rate and temperature is used in future models of *E. huxleyi* bloom formation.

5.2 Introduction

Palaeoceanographic proxies based on both the organic and inorganic remains of the oceanic coccolithophore alga *Emiliania huxleyi* are widely used for reconstructing past sea-surface conditions such as temperature (Prahl and Wakeham 1987) and salinity (Bollmann and Herrle 2007). It is often assumed that a sedimentary proxy signal reflects an average of annual sea-surface conditions. However, strictly speaking this is not always likely to be the case, as a large proportion of *E. huxleyi* production typically occurs in a single seasonal bloom event (Bijma et al. 2001; Thomsen et al. 1998). Therefore, knowledge of when and why blooms are likely to occur is needed to estimate whether the signal reflects, for example, summer or annual sea-surface temperature from the sedimentary proxy signal.

Current attempts to elicit factors controlling bloom-formation model the behaviour of *E. huxleyi* populations in response to combinations of external parameters such as temperature and nutrients (e.g. Merico et al. 2004). This approach relies on having first quantified how *E. huxleyi* population growth responds to each individual parameter. Calculations of *E. huxleyi* growth rate as a function of sea-surface temperature are based on the Eppley curve (Eppley 1972) which describes the maximum attainable growth rates of photosynthetic algae across a range of temperatures. The Eppley curve is an exponential function taking the form,

$$\mu_{max} = 0.59e^{0.0633T}$$

where, μ_{max} is the maximum potential growth rate (d^{-1}) and T is temperature (°C). A recent update of this equation, using improved statistical methods, has yielded a similar response (Bissinger et al. 2008). However, while this relationship may apply to photosynthetic

algae in general, individual species generally have a growth rate – temperature response following either a linear or a power function (Montagnes et al. 2003). Therefore, the use of the Eppley curve for modelling how *E. huxleyi* grows in response to temperature may be inappropriate.

This study aims to quantify the relationship between maximum potential growth rate and temperature for *E. huxleyi*. To achieve this, a large dataset is compiled from literature culture studies of *E. huxleyi* where both growth rate and temperature were measured. Subsequently, a combination of quantile regression and Akaike's Information Criterion (AIC) (Akaike 1974) is used to determine the model which best describes the relationship between growth rate and temperature.

5.3 Methods

5.3.1 Data collection

E. huxleyi growth rate data (n = 1051) were obtained from culture experiments detailed in the primary literature where culture temperature data were also recorded. Where data were only presented graphically they were extracted using *xyExtract* 5.1. All growth rates were converted to specific growth rate (μ, d^{-1}). All temperatures were converted to Celsius (°C).

5.3.2 Quantile regression

Quantile regression (Koenker and Bassett 1978) was used to estimate the maximum growth rate of *E. huxleyi* as a function of temperature. Calculating regression parameters for the 99^{th} quantile allows the shape of the upper edge of the dataset (i.e. maximum growth rate) to be quantified. The size of the dataset used here is large enough to allow

calculation of this quantile; it has been suggested (Rogers 1992) that n should be greater than [5 / (1 - q)], where q is the quantile (in this case 0.99 or 99th quantile). Quantile regression was calculated using *R* 2.11.1 with the `quantreg` 4.50 package.

5.3.3 Model selection

Linear and non-linear models were fitted to the 99th quantile of the data and were then compared using Akaike's Information Criterion (AIC) (Akaike 1974),

$$\mathrm{AIC} = 2p - 2L_m$$

where p is the number of parameters in the model and L_m is the maximized log-likelihood.

5.4 Results

Literature *E. huxleyi* culture data were derived from 84 publications, detailing 64 strains from 24 different locations (Fig. 5.1), of which only 6 are in the southern hemisphere, 7 are in the Pacific Ocean sector, one is in the Indian Ocean sector, two are in the Mediterranean, and 14 are in the Atlantic Ocean sector. Strains were grown under a range of light intensities (4 – 1160 μmol photons m^{-2} s^{-1}) and day-lengths (between 12 and 24 h light per day) although detailed supporting data were not available for many studies. A small proportion (~6%) of the data was derived from nutrient-limited cultures (e.g. chemostats).

Maximum *E. huxleyi* specific growth rate (μ) generally increases with temperature between 2°C and 27°C (Fig. 5.2A). There are no data below 2°C and very few data (~3) above 27°C. However, above 27°C growth rates are dramatically reduced and approach 0 d^{-1}. Maximum growth rate at any temperature was ~ 2.0 d^{-1}, although the actual value is

more likely closer to 1.9 d^{-1}. The highest growth rates are anomalous and do not conform to the general μ – temperature trend (Fig. 5.2A). These two anomalous data are from an isolated study and were excluded from subsequent analysis.

AIC selected a power function as the model which best described the 99th quantile of the response of μ to temperature (Table 5.1; Fig. 5.2A), while linear and exponential functions had similarly low AIC scores.

5.5 Discussion

5.5.1 Growth rate response to temperature

This study represents the first synthesis of data on *E. huxleyi* growth rate response to temperature. It improves on previous attempts to quantify a relationship between *E. huxleyi* growth rate and temperature which have been based on individual strains. Further, it has been shown that individual strains have different growth rate tolerances to temperature (Brand 1981) making extrapolation of strain-specific data to hypothetical scenarios such as models difficult. However, the data presented here provide a μ_{max} – temperature response which is globally applicable, as the data are derived from diverse geographic locations (Fig. 5.1).

The maximum growth rate observed here (~1.9 d^{-1}; Fig. 5.2A) confirms that *E. huxleyi* is the fastest growing coccolithophore, as can be expected due to its small size (size and maximum species growth rates being inversely proportional (Banse 1976)). The closely related *Gephyrocapsa oceanica* is similarly small but only has a maximum growth rate of around 1 d^{-1} (Buitenhuis et al. 2008; Schouten et al. 2006). Larger coccolithophores such as *Calcidiscus leptoporus* and *Syracosphaera pulchra* have much lower maximum

growth rates of below ~0.5 d^{-1} (Buitenhuis et al. 2008). The fast growth rate of *E. huxleyi* in relation to other coccolithophores, combined with its wide temperature tolerance, is likely to be a factor in bloom formation.

5.5.2 Implications for modelling *E. huxleyi* blooms

Previously, models of *E. huxleyi* bloom formation have assumed that maximum growth rate is exponentially related to temperature following the multi-species study of Eppley (1972). However, quantile regression analysis in this study has shown that the relationship is better described by a power or a linear function (Table 5.1; Fig. 5.2A). Power and linear μ – temperature response curves were shown to be the norm for individual species of photosynthetic algae, whereas no exponential relationships were observed (Montagnes et al. 2003). Figure 5.2B shows the difference between growth rate estimation using the power function from this study and using the two multi-species exponential curves, the original (Eppley 1972) and the recently updated (Bissinger et al. 2008). In both cases the difference between the power and exponential functions is largest at extremes of temperature, and smallest between around 10 and 15°C. At 15°C the power function presented in this study gives a specific growth rate 40% lower than that given by the exponential response of Bissinger et al. (2008). This difference widens to around 50% at both 5 and 25°C (Fig. 5.2B). Although the majority of *E. huxleyi* blooms occur in waters with mean annual sea-surface temperatures of between around 3 and 15°C (Iglesias-Rodriguez et al. 2002) an exponential growth rate response to temperature is still likely to overestimate maximum growth rate.

A key aspect of determining the success of an *E. huxleyi* bloom lies in *E. huxleyi* growth rate relative to that of its grazers. It has been hypothesised that photosynthetic algal blooms occur more frequently in temperate latitudes than in other regions due to the

ability of photosynthetic bloom species to grow faster at these temperatures than can their grazers (Rose and Caron 2007). Small changes in growth rate parameters of *E. huxleyi* at these temperatures (i.e. <15°C) would have a large impact on whether their grazers would be able to outperform them. Therefore, it is recommended that in future models of *E. huxleyi* bloom formation the power function presented in this study be used for relating maximum *E. huxleyi* growth rate to temperature (Table 5.1).

5.5.3 Potential sources of error

The growth rate – temperature dataset in this study is the largest and most comprehensive yet to be made of *E. huxleyi*. However, the data are potentially complicated by sampling bias. As is fairly evident from Figure 5.2A, there are a large number of data at 15 and 20°C. This is likely due to two reasons. First, these provide high growth rates approaching that of the optimum growth temperature (~25°C). High growth rates are desirable in laboratory culture experiments simply because they allow experiments to be conducted in a shorter space of time. Second, 15 – 20°C is the approximate range of temperate latitude summer sea-surface temperatures, from which many strains will have been isolated. Third, 15 and 20°C are from the psychology of the experimenter, easier to aim for than are, for example, 14 and 19°C. In this instance the accuracy of these temperatures may be called into question. Most culture studies do not provide temperature error estimates, but these likely vary by at least ±1°C. However, even with the existence of temperature errors such as these the general μ – temperature relationship would likely be broadly similar.

A further source of error may be derived from a biased distribution of other growth rate-regulating effects such as photon flux density. However, data for nutrient

concentration, salinity, and photon flux density were incomplete and as such it is difficult to separate the effects of these variables.

5.5.4 Conclusions

In this study, the relationship between the maximum growth rate of *E. huxleyi* and temperature has been quantified. A power function best described the 99th quantile of the data, while a linear function was almost as powerful; both functions described the growth rate response better than an exponential equation. These results provide improved parameters for the determination of *E. huxleyi* growth rate compared to the previously used exponential function (Eppley 1972). It is recommended that these parameters (Table 5.1) are used for any future modelling of *E. huxleyi* bloom formation.

Table 5.1. Model parameters and AIC scores for the five models which best fit the data in Fig. 5.2A.

			Parameters			
Model	**AIC**	**Equation**	***n***	***a***	***b***	***c***
Power	11.82	$a \times (T^b)$	2	0.1240	0.8537	-
Linear	11.85	$a \times T + b$	2	0.0720	0.1600	-
Exponential	12.05	$a \times e^{(b \times T)}$	2	0.6813	0.0426	-
Quadratic	13.75	$a + (b \times T) + (c \times T^2)$	3	-0.0933	0.1172	-0.0016
Flinn	13.80	$1/(1 + a + (b \times T) + (c \times T^2))$	3	0.8863	-0.1013	0.0019

Table 5.2. *E. huxleyi* strains used in this study with their original isolation coordinates and references to the studies which provided growth rate and temperature data for each strain.

Strain	Latitude	Longitude	Reference
88E	42	-68	(Balch et al. 1996a; Balch et al. 1992; Fernandez et al. 1996b; Fritz 1999; Fritz and Balch 1996; Keller et al. 1999b; Merrett et al. 1993; Nimer et al. 1994; Price et al. 1998)
89E	42	-68	(Bidle et al. 2007; Bucciarelli et al. 2007; Dyhrman and Palenik 2003; Popp et al. 2006; Shaked et al. 2006; Steinke et al. 1998; Stoll et al. 2002b; Sunda et al. 2007; Wolfe et al. 2002; Xu et al. 2006)
A1383			(Sunda and Huntsman 1992)
A266	42	-68	(Brand 1984)
A47	37	-67	(Brand and Guillard 1981)
A528	36	-67	(Brand 1984)
AC472			(Houdan et al. 2005)
BOF92	48	-17	(Paasche 1998; Paasche 1999; Paasche and Brubak 1994; Paasche et al. 1996)
BT-6	32.2	-64.5	(Bidigare et al. 1997; Bidle et al. 2007; Dupont et al. 2004; Dyhrman and Palenik 2003; Epstein et al. 2001; Popp et al. 2006; Popp et al. 1998a; Steinke et al. 1998; Sunda and Hardison 2007; Sunda and Huntsman 1992; Watabe and Wilbur 1966; Wolfe et al. 2002; Wong et al. 2002)
CCMP1516	-2.7	-82.7	(Dyhrman and Palenik 2003; Evans et al. 2007; Evans et al. 2006; Steinke et al. 1998)
CCMP370	59.5	10.5	(De La Cuesta and Manley 2009; Steinke et al. 1998; Wolfe et al. 2002)
CCMP371	32	-62	(Feng et al. 2008)
CCMP376	42	-68	(Matrai and Keller 1994)
Ch24-90	57	1	(Buitenhuis et al. 1999; Van Bleijswijk et al. 1994; Van Bleijswijk and Veldhuis 1995)
Ch25-90	57	1	(Van Bleijswijk and Veldhuis 1995)
CS-369	-42.9735	147.5242	(Guan and Gao 2010)
EH2	-18	147	(Sorrosa et al. 2005)
F	60	11	(Paasche 1967; Paasche and Klavenes.D 1970)
F61	60	11	(Paasche 1998; Paasche et al. 1996)
L	60	11	(Buma et al. 2000; Page et al. 1999; Riegman et al. 2000; Steinke et al. 1998; Stolte et al. 2000; Van Bleijswijk and Veldhuis 1995; Van De Poll et al. 2007; Van Rijssel and Gieskes 2002)
M	66	2	(Mjaaland 1956)
MCH1	37	-67	(Brand 1984)

NAP9	40.5	13.5	(Paasche 1999)
NEPCC 55	48	-130	(Brand 1984)
NEPCC 55a	50	-145	(Conte et al. 1998; Epstein et al. 2001; Popp et al. 2006; Prahl et al. 2003; Price et al. 1998)
NEPCC 646	60	11	(Price et al. 1998)
NEPCC 732	50	-145	(Needoba and Harrison 2004; Needoba et al. 2003)
Nervion River Estuary	43.3	-3	(Seoane et al. 2009)
OF8	60	11	(Paasche et al. 1996)
own isol	50	-145	(Thompson and Calvert 1995)
own isol Muggli (see NEPCC732)	50	-145	(Lecourt et al. 1996)
own isol.	59.5	10.5	(Garde and Cailliau 2000)
own isol.	50	-145	(Muggli and Harrison 1996a; Muggli and Harrison 1996b; Varela and Harrison 1999)
P3			(Mjaaland 1956)
P8			(Mjaaland 1956)
PLY 92/92D	50.2	-6	(Boye and Van Den Berg 2000; Leal et al. 1999; Takano et al. 1995; Vasconcelos et al. 2002)
PLY 92A	50.2	-4.25	(Steinke et al. 1998; Wolfe et al. 2002)
PLY B317	60	5	(Nielsen 1997; Paasche et al. 1996)
PLY B92/11	60	5	(Bidigare et al. 1997; Conte et al. 1998; Langer et al. 2006; Langer et al. 2007; Langer et al. 2009b; Leonardos and Harris 2006; Paasche et al. 1996; Popp et al. 1998a; Rickaby et al. 2002; Riebesell et al. 2000; Rost et al. 2002; Schouten et al. 2006; Schulz et al. 2007)
PLY D53/74/6	24	-20	(Paasche et al. 1996)
PLY D61	61	-20	(Paasche et al. 1996)
PLY G1779	60	-20	(Paasche et al. 1996)
PLY G1779Ga	60	-20	(Conte et al. 1998)
PLY M181	32	-62	(Conte et al. 1998; Paasche et al. 1996)
PLY M219	-47	-168	(Rhodes et al. 1995)
Populations D – U (except O) (17 strains)	37	-67	(Brand 1982)
SAF	-30	30	(Conte et al. 1998; Paasche et al. 1996)
SC91	58	9	(Paasche 1999; Paasche et al. 1996)
TQ26DIP	-42	170	(Buitenhuis et al. 2008)
TW1 / AC474			(Sciandra et al. 2003)

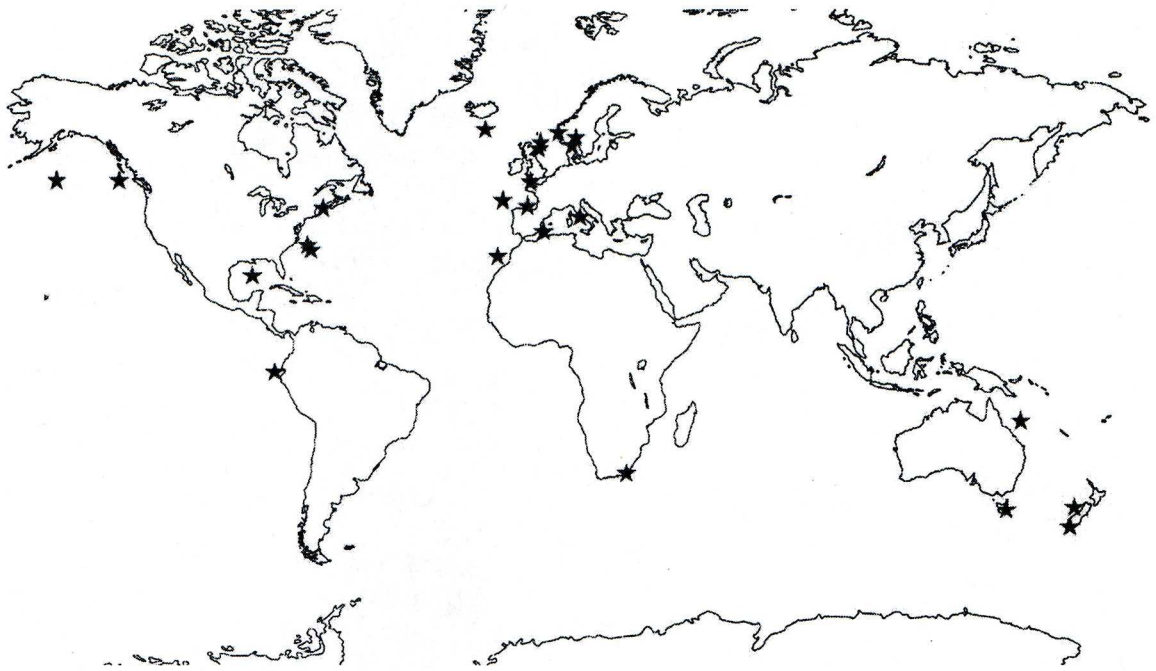

Fig. 5.1. Geographical locations of *E. huxleyi* strains used in literature data compiled in this study.

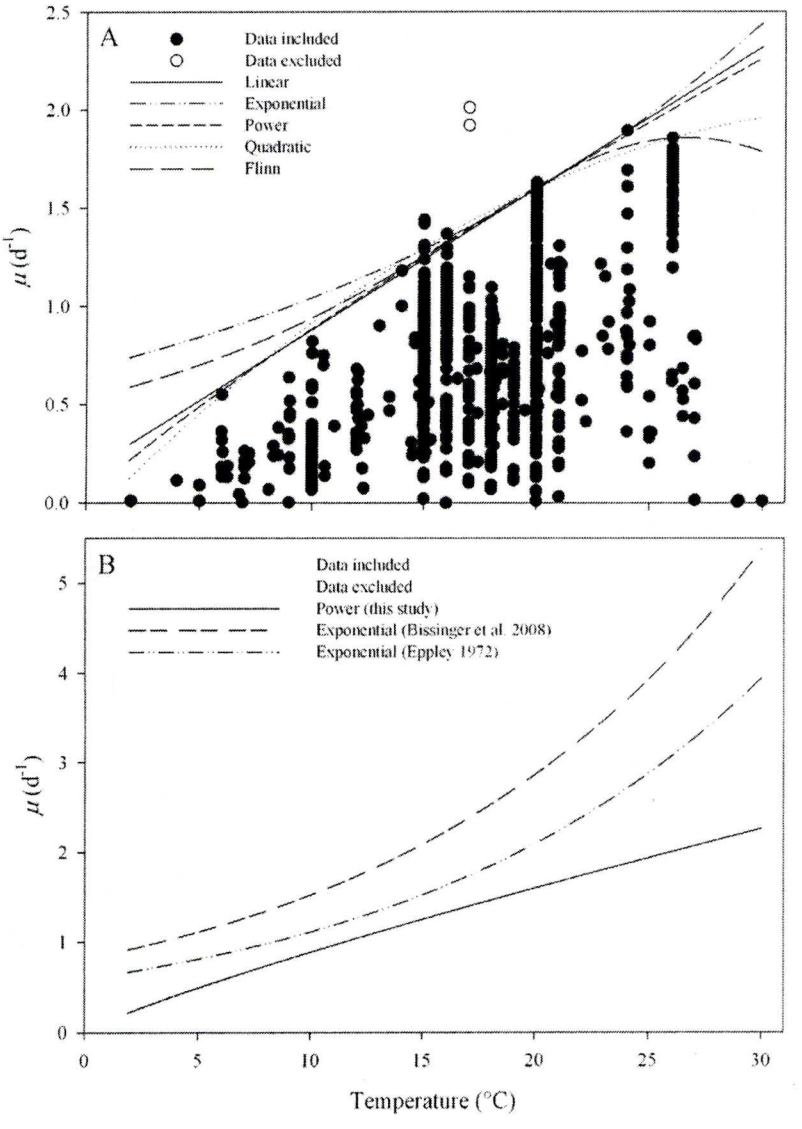

Fig. 5.2. (A) *E. huxleyi* specific growth rate (μ) as a function of temperature. Data were compiled from the literature. Linear, exponential, power, quadratic, and Flinn curves fit to the 99th quantile of the data (except for 2 data; see figure legend); see Table 5.1 for parameters. (B) Power function from Fig. 5.2A compared to the original (Eppley 1972) and updated (Bissinger et al. 2008) exponential functions. Note different *y*-axes.

6 Elevated coccolithophore production of dimethylsulphoniopropionate at high salinities

6.1 Abstract

The relationship between *E. huxleyi* dimethylsulphoniopropionate and salinity was quantified using culture experiments and gas chromatographic analysis. The DMSP content of two open-ocean strains of *E. huxleyi* displayed positive linear responses to salinity while a strain from a marginal environment displayed a non-linear response. This geographical divide suggests that open-ocean strains are genetically different to those in marginal settings as has been observed for *E. huxleyi* coccolith morphology. The relationship between open-ocean DMSP content and salinity suggests that net *E. huxleyi* DMSP is likely to have increased in all ocean basins at the Last Glacial Maximum except for the North Atlantic where salinity decreased. This potential basin scale difference in DMSP production is partly reflected in ice core records of sulphate aerosols from both Greenland and Antarctica.

6.2 Introduction

The control of atmospheric air temperature is a key aspect of climate change in both the past and future. One factor that can affect air temperature is the existence of sulphur aerosols in the stratosphere (Dickinson and Cicerone 1986). These aerosols not only scatter incoming solar radiation but also reflect it due to their role in cloud formation as cloud condensation nuclei (Malin et al. 1992). A major source of atmospheric sulphur aerosols is the marine biogenic compound dimethylsulphide (DMS), which is derived from dimethylsulphoniopropionate (DMSP). DMSP is biosynthesised primarily as a compatible solute to control osmotic regulation by marine algae, including the coccolithophores, which have notably high intracellular DMSP concentrations compared to most other phytoplankton groups (Malin and Steinke 2004). Atmospheric biogenic DMS concentration is controlled by (i) phytoplankton DMSP production, (ii) its conversion to DMS, and (iii) its flux from the ocean to the atmosphere (Simo 2001).

The link between DMS and climate remains poorly understood. Sulphur aerosol records from Antarctic and Greenland ice-cores over the past ~100 ka have revealed changes in atmospheric DMS in concert with global climate change (e.g. Hansson and Saltzman 1993; Legrand et al. 1991). However, analysis has been inconclusive, with results suggesting higher atmospheric DMS in both glacial and interglacial periods, depending on the core location. Other attempts to understand what drives atmospheric DMS have tried to reveal controls on DMSP production in the ocean. Recent focus has been on the DMSP response of the globally distributed and abundant coccolithophore *Emiliania huxleyi* to (i) temperature (Van Rijssel and Gieskes 2002), (ii) concentrations of CO_2 (Vogt et al. 2008), and (iii) nutrients (Sunda et al. 2007). However, although sea surface salinity (SSS) has varied significantly over glacial-interglacial cycles (Wolff et al.

1999), little attention has been paid to the potential DMSP response of *E. huxleyi* to changes in salinity.

Elevated salinity is known to cause increased cellular DMSP content across a range of algal groups (Dickson and Kirst 1987a; Dickson and Kirst 1987b; Vairavamurthy et al. 1985). However, the species used for these studies have either restricted spatial distributions or abundances. However, for the bloom-forming and widespread *E. huxleyi*, a relationship between salinity and DMSP has not yet been confirmed, let alone quantified.

In this study, the response of *E. huxleyi* DMSP to salinity is investigated using culturing techniques across a range of experimental salinities which encapsulates the SSS of both present and glacial oceans.

6.3 Methods

6.3.1 Culturing

E. huxleyi strains PLY B92/11 (coastal Norway), RCC 948 (south-east Pacific), and RCC 962 (central Pacific) were grown in semi-continuous batch culture (Brand et al. 1981) in 250 mL Erlenmeyer flasks, each filled with artificial seawater (ASW), at ~175 μmol photons m^{-2} s^{-1} continuous light and at 18°C. ASW was made using deionized water, synthetic sea salt (Ultramarine, Waterlife Research Industries), f/2 nutrient-enrichment media (Sigma, G0154; (Guillard 1975)), and Na_2SeO_3 to a final concentration of 10 nmol L^{-1} (Danbara and Shiraiwa 1999). ASW was sterilised by filtration at 0.2 μm and salinities were determined using an Autosal 8400 (Guildline Instruments).

6.3.2 DMS and DMSP experiments and analysis

Cultures were grown at 8 salinities between 30 and 44 and were acclimated to each treatment for >10 generations before being sub-cultured into experimental flasks (Fielding et al. 2009). Throughout acclimation and experimentation, cultures were re-suspended twice daily and maintained in exponential growth phase at concentrations below 3.0×10^4 cells mL^{-1} to avoid large changes in the aqueous carbonate system. Samples were taken in exponential growth phase for DMSP and DMS analysis (performed by Michael Steinke at the University of Essex).

For each treatment, one 3 mL sample for particulate DMSP ($DMSP_p$) analysis was filtered through a pre-combusted (500°C, 24 h) Whatman GF/F under <5 kPa to minimise cell lysis. The filter was then immediately placed in 3 mL (0.5 mol L^{-1}) NaOH. To measure cellular leakage of DMSP and conversion of DMSP to DMS an additional 2.85 mL sample for total dissolved and particulate DMSP and DMS ($DMSP_t$) was taken and directly added to 150 μL (10 mol L^{-1}) NaOH to give a final concentration of 0.5 mol L^{-1} NaOH (NaOH addition causes alkaline hydrolysis of all DMSP to DMS). To calculate concentrations of $DMSP_p$ and $DMSP_t$ per cell, culture cell concentrations were measured using a CASY electronic particle counter (Innovatis). $DMSP_p$ and $DMSP_t$ samples were stored at room temperature in septum-capped Finneran vials prior to analysis. Samples were incubated for 24 h at 30°C and then analysed using gas chromatography and flame photometric detection (Shimadzu GC-2010 with a 30 m, 0.53 mm CP-Sil 5CB capillary column). *See* Appendix 6.1 for all raw data. Standard deviation within each treatment was under 0.08 fmol $DMSP_t$ $cell^{-1}$ and under 0.06 fmol $DMSP_p$ $cell^{-1}$. As the shapes of the relationships between salinity and DMSP were not known it is recommended that replication should be made by maximising the number of environmental treatments (i.e. at

different salinities) rather than within each of a smaller number of treatments (Montagnes and Berges 2004).

6.3.3 Statistical analysis

Least squares regressions of $DMSP_p$ and $DMSP_t$ as a function of salinity were applied to each strain. Slope and intercepts of linear regressions were compared to determine between-strain differences (*t*-test; $\alpha = 0.05$).

6.4 Results

$DMSP_p$ per cell is significantly related to salinity for all strains (Fig. 6.1A). The two open ocean Pacific strains (RCC 948 and 962) displayed linear relationships to salinity ($r^2 = 0.90$ and 0.55 respectively), while the coastal Norwegian strain (PLY B92/11) followed a quadratic response ($r^2 = 0.90$). The intercept of RCC 948 (S.E. Pacific) is significantly higher than that of RCC 962 (central Pacific).

$DMSP_t$ is related to salinity in an identical way for each strain although $DMSP_t$ was consistently higher than $DMSP_p$ by 1.42±1 fmol $cell^{-1}$ (Fig. 6.1B). The linear regression for the $DMSP_t$ of RCC 962 has a higher r^2 (0.74) than that for $DMSP_p$.

6.5 Discussion

6.5.1 Salinity – DMSP response between strains

The results of this study show that, like many other phytoplankton species (Dickson and Kirst 1987a; Dickson and Kirst 1987b), DMSP content of *E. huxleyi* generally increases with increasing salinity (Fig. 6.1). For the two open ocean Pacific strains $DMSP_t$

increases by between 0.28 and 0.49 fmol $cell^{-1}$ per unit salinity. However, the results presented here also highlight significant between-strain variability in cellular DMSP of up to ~2.5 fmol $cell^{-1}$ at higher salinities. The near identical response to salinity observed with both $DMSP_p$ and $DMSP_t$ (Fig. 6.1) shows that differences between strains are not due to leakage of DMSP from the cell or from conversion of DMSP to DMS. While SSS change will exert an effect on total DMSP production, a shift in strain dominance in ocean surface waters has the potential to override this effect.

Reduced DMSP per cell at the highest salinities in the strain from coastal Norway reflects a further intra-species difference. A similar depression of DMSP content at higher salinities was observed for cultures of the estuarine diatom *Cylindrotheca closterium* (Van Bergeijk et al. 2003), but not for the open ocean coccolithophore *Pleurochrysis carterae* (Vairavamurthy et al. 1985). This suggests that strain provenance may play a role in determining the linearity of the salinity – DMSP response. The generally lower salinity in estuarine and other coastal environments (often as low as 31 in coastal Norwegian waters (Batvik et al. 1997)) due to freshwater input may have caused coastal species to have lost the ability to synthesise enough DMSP to tolerate the higher salinities present in the open ocean (32 – 37 (Antonov et al. 2006)). A genetic difference between open-ocean and coastal strains of *E. huxleyi* has previously been observed for cell physiological and biochemical characteristics (Conte et al. 1995; Fielding et al. 2009; Paasche 2002). Alternatively, Van Bergeijk *et al.* (2003) noted that, at higher salinities, the amino acid proline became the dominant compatible solute in place of DMSP, which suggests that coastal strains may have evolved a different response pathway to salinity change.

6.5.2 Last Glacial Maximum DMSP production

Understanding drivers of the production of DMSP by phytoplankton such as *E. huxleyi* is pertinent to assessing the interaction of atmospheric sulphur with past climate. Due to different patterns of precipitation, evaporation, and ocean circulation, SSS at the Last Glacial Maximum (LGM) was considerably different to that today. In the Pacific, Indian and Southern Oceans SSS was ~1 unit higher than it is at present, while LGM SSS in the northern Atlantic was up to 4 units lower (Kim et al. 2003).

The experimental results presented in this paper, combined with knowledge of LGM SSS, suggest that coccolithophore DMSP is likely to have increased in all ocean basins except for the Atlantic. Increased concentrations of atmospheric methanosulphonate (MSA; an oxidation product of DMS) has been linked to the presence of *E. huxleyi* (Kubilay et al. 2002). Indeed, ice core records of MSA from Greenland suggest lower glacial DMSP production over the North Atlantic (Hansson and Saltzman 1993; Legrand et al. 1997; Saltzman et al. 1997). This is in contrast to the majority of data from the southern hemisphere which show elevated glacial DMSP (Legrand et al. 1991; Saigne and Legrand 1987). However, linking basin-scale DMSP production with ice core records of MSA should be made with caution as MSA deposition relies on a variety of factors such as local sea-ice extent (Rhodes et al. 2009), changing sources of moisture advection (Preunkert et al. 2008), and pre- and post-depositional effects (Simo 2001; Traversi et al. 2009). Nonetheless, the discrepancy in MSA deposition between hemispheres may be partly explained by the freshening of the North Atlantic during the LGM, and thus a net decrease in localised production of DMSP.

6.5.3 Other variables affecting *E. huxleyi* DMSP

At the LGM sea-surface temperature (SST), nutrient cycling, and solar insolation were different to those at present (Climap 1981). For example, SST was considerably lower by up to ~4°C in the Southern and Pacific Oceans, and by up to ~6°C in the North Atlantic (Locarnini et al. 2006). Previous culture work has highlighted environmental factors other than salinity which can affect *E. huxleyi* DMSP. Keller (1999b) found that nitrogen limitation caused a small decrease in $DMSP_p$ by ~0.5 fmol $cell^{-1}$, while van Rijssel & Gieskes (2002) found that light limitation decreased $DMSP_p$ by ~2.5 fmol $cell^{-1}$. However, the same study also found decreasing temperature led to increased $DMSP_p$ by ~23 fmol $cell^{-1}$ (Van Rijssel and Gieskes 2002). Below 15°C $DMSP_p$ decreased at a rate of ~1.6 fmol $cell^{-1}$ per 1°C. The salinity increase in this study, however, only causes $DMSP_p$ to increase by up to ~5 fmol $cell^{-1}$ at a rate of up to ~0.49 fmol $cell^{-1}$ per unit salinity (Fig. 6.1A; south-east Pacific strain).

When the difference in SSS and SST are translated into difference in DMSP between the LGM and present, the effect caused by temperature change is about ten times that of salinity. In the Southern and Pacific Oceans the temperature and salinity change at the LGM would equate to +6.40 and +0.49 fmol DMSP $cell^{-1}$ respectively. The North Atlantic should experience +9.60 fmol DMSP $cell^{-1}$ due to the 6°C decrease, and -1.96 fmol DMSP $cell^{-1}$ due to the SSS decrease of ~4. However, it should be noted that the effect of temperature on DMSP production has not been measured for open-ocean strains of *E. huxleyi*; the strain used by van Rijssel and Gieskes (2002) was from Norwegian coastal waters and could therefore be, as it is for salinity-DMSP, markedly different to open-ocean strains in its temperature-DMSP response. Further, the decrease in sea-level at the LGM (Huybrechts 2002) would likely cause a reduction of marginal habitats and the

dominance of open-ocean strains of *E. huxleyi*. Therefore, the effect of temperature on DMSP production in open-ocean strains requires testing before assumptions can be made about the relative importance of either salinity or temperature.

6.5.4 Conclusion

In this study the relationship between salinity and DMSP was quantified for *E. huxleyi* and was found to be positive and linear for open-ocean strains but non-linear and quadratic for a coastal strain. For open-ocean strains the relationship between salinity and DMSP was stable across a range of salinities encompassing those from the LGM and the present oceans. Lowered LGM SSS and consequently lowered DMSP in the North Atlantic, but not elsewhere, broadly agrees with ice core proxy records of DMSP production. However, the effect of lowered LGM temperature and changes in strain dominance may be more important factors than salinity on the amount of DMSP produced by *E. huxleyi* cells.

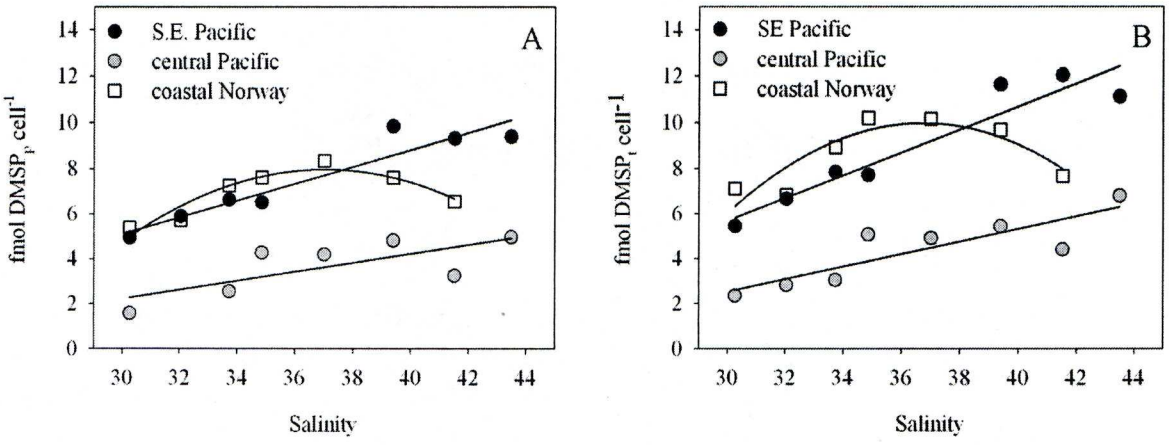

Fig. 6.1 Culture experimental results of (A) particulate DMSP ($DMSP_p$), and (B) the sum of dissolved and particulate DMS and DMSP ($DMSP_t$) as a function of salinity for one coastal and two open-ocean strains of the coccolithophore *Emiliania huxleyi*.

---Intentionally blank---

Appendix 6.1. Raw data used to calculate $DMSP_p$ and $DMSP_t$ per cell.

Strain	S	Cell concentration (cells mL^{-1})	Cell volume (μm^3)	$DMSP_p$ (nmol)	$DMSP_t$ (nmol)
S.E. Pacific	30.26	70285	48.35	1.04	1.09
S.E. Pacific	32.04	62695	55.06	1.11	1.19
S.E. Pacific	33.73	107300	46.14	2.14	2.40
S.E. Pacific	34.86	92140	56.83	1.80	2.03
S.E. Pacific	37.01	59670	41.63		
S.E. Pacific	39.39	137350	43.25	4.06	4.56
S.E. Pacific	41.52	108650	50.97	3.04	3.73
S.E. Pacific	43.49	71470	47.71	2.01	2.27
central Pacific	30.26	45780	55.06	0.22	0.31
central Pacific	32.04	30675	54.54		0.25
central Pacific	33.73	54185	38.93	0.41	0.47
central Pacific	34.86	80980	40.19	1.04	1.17
central Pacific	37.01	41365	45.52	0.52	0.58
central Pacific	39.39	74815	44.45	1.08	1.16
central Pacific	41.52	46197	50.30	0.45	0.58
central Pacific	43.49	49545	63.31	0.74	0.96
coastal Norway	30.26	52940	51.63	0.86	1.07
coastal Norway	32.04	27970	50.47	0.48	0.55
coastal Norway	33.73	68795	42.95	1.50	1.75
coastal Norway	34.86	107850	49.00	2.46	3.13
coastal Norway	37.01	37945	37.69	0.95	1.10
coastal Norway	39.39	67000	42.36	1.53	1.85
coastal Norway	41.52	35105	46.77	0.69	0.77

(Appendix 6.1 contd...)

fmol $DMSP_p$ $cell^{-1}$	fmol $DMSP_p$ μm^{-3} cell $volume^{-1}$ $cell^{-1}$	fmol $DMSP_t$ $cell^{-1}$	fmol $DMSP_t$ μm^{-3} cell $volume^{-1}$ $cell^{-1}$
4.94	0.10	5.46	0.11
5.90	0.11	6.67	0.12
6.64	0.14	7.84	0.17
6.51	0.11	7.72	0.14
9.84	0.23	11.65	0.27
9.32	0.18	12.05	0.24
9.39	0.20	11.13	0.23
1.58	0.03	2.35	0.04
		2.83	0.05
2.55	0.07	3.06	0.08
4.27	0.11	5.08	0.13
4.19	0.09	4.92	0.11
4.82	0.11	5.45	0.12
3.25	0.06	4.41	0.09
4.97	0.08	6.81	0.11
5.39	0.10	7.12	0.14
5.72	0.11	6.84	0.14
7.25	0.17	8.93	0.21
7.60	0.16	10.19	0.21
8.35	0.22	10.15	0.27
7.61	0.18	9.69	0.23
6.55	0.14	7.67	0.16

7 Concluding discussion

7.1 Summary

This thesis addresses several palaeoceanographic proxies and processes related to *E. huxleyi*; namely, palaeo-SSS (2), palaeo-sea-surface CO_2 (3), palaeo-productivity (4), bloom formation (5), and DMSP production (6). Each chapter takes a different approach, either generating original data, or using the large amount of data available in the literature. The results highlight the ability of culture experiment data to address questions that may otherwise be unapproachable from the perspective of *in situ* oceanographic data collection.

In the chapters addressing palaeoenvironmental proxies (2, 3, and 4), the results generally support the current application of each proxy, while adding caveats or updated error estimates for application. Chapter 5 does not directly address a proxy but provides improved parameter-estimates for models which seek to determine the causes and effects of bloom formation; a process which is regionally important in contributing to *E. huxleyi* proxy signals (Bijma et al. 2001). Chapter 6 quantifies the effect of a hitherto-unaddressed biogeochemical process (salinity – *E. huxleyi* DMSP) which could potentially affect the global S cycle and thus climate.

Chapter 2 highlights biogeographical constraints on the application of the palaeo-SSS proxy that was originally proposed by Bollmann & Herrle (2007). Analysis shows that use of the proxy in marginal and isolated regions of the ocean, such as Norwegian coastal waters, the Black Sea, and the Red Sea, should be made with caution. These results recommend that a localised relationship between SSS and *E. huxleyi* coccolith morphology should be made for each of these locations before application as a proxy.

Chapter 3 updates previous estimates of palaeo-sea surface CO_2 by providing a significantly larger sample size for determining one of the proxy's input parameters, cell volume to surface area ratio (V:SA). Contrary to analysis of *E. huxleyi* coccolith morphology, neither salinity nor biogeographical location can explain variation in *E. huxleyi* cell V:SA. The temporal patterns of revised estimates of CO_2 do not differ greatly from those made previously (Henderiks and Pagani 2007). However, these results highlight that an additional error exists of between 6 and 30 μmol CO_2 kg^{-1} from the middle Eocene and the early Miocene. This represents an approximate doubling of the original error estimates and should be taken into account when reconstructing palaeo-sea surface CO_2 using this method.

Chapter 4 highlights bloom formation as a mechanism for potentially controlling the Sr/Ca of *E. huxleyi* coccoliths. Coccolith Sr/Ca is currently concluded to be controlled by the rate at which coccoliths are produced (Stoll et al. 2002b). However, the results in this chapter do not refute the use of *E. huxleyi* Sr/Ca as a palaeoproductivity proxy, but merely suggest that it may reflect the occurrence of bloom events as opposed to palaeoproductivity *per se*. However, the theoretical approach used in this chapter would require ground-truthing before any solid conclusions could be made about the interpretation of *E. huxleyi* coccolith Sr/Ca.

Chapter 5 improves on previous estimates of *E. huxleyi* growth rate in response to changing SST. This chapter proposes a power relationship between temperature and *E. huxleyi* maximum growth rate as opposed to the conventional multi-species exponential response (Bissinger et al. 2008; Eppley 1972). An attempt to quantify the impact of this revision on the outcome of bloom models is outside the scope of the present study. However, the difference between the revised relationship and that used previously is more

pronounced at extreme high and low temperatures. Nevertheless, the results provide a more reliable basis on which to model *E. huxleyi* bloom dynamics in the future.

Chapter 6 quantifies the effect of changing salinity on the quantity of DMSP produced by *E. huxleyi* cells. This analysis suggests that the salinity – DMSP relationship is different in coastal isolates of *E. huxleyi* than it is in open-ocean isolates. This supports the observations of a coastal – open-ocean divide in coccolith morphology (Chapter 2) (Fielding et al. 2009). Additionally, the positive relationship between salinity and DMSP might be reflected by the simultaneous freshening of the North Atlantic (Kim et al. 2003) and the decrease in atmospheric sulphate deposition over Greenland (Hansson and Saltzman 1993; Legrand 1997; Saltzman et al. 1997) at the Last Glacial Maximum. However, comparison of the effect of salinity with that of temperature suggests that SSS may only have had a secondary effect in determining sea-surface DMSP productivity in the past.

7.2 Scope for further research

Chapters 2 and 4 provide opportunities for further investigation. Understanding the divide between the SSS – coccolith morphology relationship in the open ocean and in marginal environments (Chapter 2) may benefit from further substantiation. The majority of coccolith morphology data upon which this observation was based were derived from the open-ocean and from Norwegian fjords. Therefore further culture experiments on strains of *E. huxleyi* from marginal settings such as the Black Sea and the Red Sea would help to either support or refute the hypotheses outlined here. The potential genetic divide between marginal and open-ocean populations of *E. huxleyi* is lent weight by the salinity – DMSP

results (Chapter 6), although not by cell V:SA (Chapter 3). Further, there is evidence from lipid composition (Conte et al. 1995) and growth physiology (Paasche 2002) of a marginal – open-ocean genetic divide between *E. huxleyi* populations. In the light of this body of evidence it may be pertinent to quantify the effect of biogeographical sample provenance on other proxies based on *E. huxleyi*, such as $U^{K}_{37'}$ before they are routinely applied in marginal locations.

The bloom mechanism potentially affecting coccolith Sr/Ca outlined in Chapter 3 is based purely on theory. However, this mechanism lends itself well to testing using laboratory cultures and perhaps by *in situ* bloom measurements of each of the model components. Primarily, the effect of coccolith calcite production on bulk coccolith Sr/Ca should first be quantified under laboratory settings. However, maintaining a constant coccolith calcification rate and a relatively steady-state carbonate system may prove to be prohibitive for generating reliable empirical data.

The contribution of Chapter 5 to understanding the mechanisms of *E. huxleyi* bloom formation requires testing by re-running existing models (e.g. Merico et al. 2004) using the new input parameters for growth rate. However, as there are noted differences in growth physiology between strains from different locations (Paasche 2002) it would be timely to assess the impact of biogeography (e.g. latitude, Atlantic/Pacific, N/S hemisphere divides, etc.) on the relationship between temperature and growth rate.

While the effect of the updated parameter estimates provided in Chapter 3 on reconstructions of palaeo-sea surface CO_2 have been discussed in that chapter, their integration into future CO_2 reconstructions is strongly recommended. Similarly it is recommended that where a proxy reconstruction relies on assumptions about *E. huxleyi*

physiology, morphology, or chemistry, these assumptions should ideally be tested using the large archive of available literature data before routine proxy application.

8 References

Akaike, H. 1974. A new look at statistical-model identification. IEEE Transactions on Automatic Control **AC19:** 716-723.

Andersen, N. R., J. D. Gassaway, and W. E. Maloney. 1970. Relationship of strontium - chlorinity ratio to water masses in tropical Atlantic-Ocean and Caribbean-Sea. Limnol. Oceanogr. **15:** 467-&.

Andersen, N. R., and D. N. Hume. 1968. Determination of barium and strontium in sea water. Anal. Chim. Acta **40:** 207-&.

Andreae, M. O., and P. J. Crutzen. 1997. Atmospheric aerosols: Biogeochemical sources and role in atmospheric chemistry. Science **276:** 1052-1058.

Antonov, J. I., L. R. A., B. T. P., M. A. V., and G. H. E. 2006. World Ocean Atlas 2005, Volume 2: Salinity. *In* L. S. [ed.], NOAA Atlas NESDIS 62.

Atkinson, D., B. J. Ciotti, and D. J. S. Montagnes. 2003. Protists decrease in size linearly with temperature: ca. 2.5% degrees C^{-1}. P. Roy. Soc. B.-Biol. Sci **270:** 2605-2611.

Balch, W. M., J. Fritz, and E. Fernandez. 1996a. Decoupling of calcification and photosynthesis in the coccolithophore *Emiliania huxleyi* under steady-state light-limited growth. Mar. Ecol.-Prog. Ser. **142:** 87-97.

Balch, W. M., P. M. Holligan, and K. A. Kilpatrick. 1992. Calcification, photosynthesis and growth of the bloom-forming coccolithophore *Emiliania huxleyi*. Continental Shelf Research **12:** 1353-1374.

Balch, W. M., K. A. Kilpatrick, P. Holligan, D. Harbour, and E. Fernandez. 1996b. The 1991 coccolithophore bloom in the central North Atlantic .2. Relating optics to coccolith concentration. Limnol. Oceanogr. **41:** 1684-1696.

Balch, W. M., A. J. Plueddeman, B. C. Bowler, and D. T. Drapeau. 2009. Chalk-Ex-Fate of CaCO3 particles in the mixed layer: Evolution of patch optical properties. J. Geophys. Res. **114:** 29.

Banse, K. 1976. Rates of growth, respiration and photosynthesis of unicellular algae as related to cell-size - review. J. Phycol. **12:** 135-140.

Batvik, H., B. R. Heimdal, K. M. Fagerbakke, and J. C. Green. 1997. Effects of unbalanced nutrient regime on coccolith morphology and size in *Emiliania huxleyi* (Prymnesiophyceae). Eur. J. Phycol. **32:** 155-165.

Beaufort, L., I. Probert, and N. Buchet. 2007. Effects of acidification and primary production on coccolith weight: Implications for carbonate transfer from the surface to the deep ocean. Geochem. Geophys. Geosyst. **8**.

Berge, G. 1962. Discoloration of the sea due to *Coccolithus huxleyi* "bloom". Sarsia **6:** 27-41.

Bernat, M., C. J. Allegre, and T. Church. 1972. Barium and strontium concentrations in Pacific and Mediterranean sea-water profiles by direct isotope dilution mass-spectrometry. Earth Planet. Sci. Lett. **16:** 75-80s.

Bidigare, R. R. and others 1997. Consistent fractionation of ^{13}C in nature and in the laboratory: Growth-rate effects in some haptophyte algae. Global Biogeochem. Cy. **11:** 279-292.

Bidle, K. D., L. Haramaty, J. B. E. Ramos, and P. Falkowski. 2007. Viral activation and recruitment of metacaspases in the unicellular coccolithophore, Emiliania huxleyi. Proc. Natl. Acad. Sci. U. S. A. **104:** 6049-6054.

Bijma, J. and others 2001. Primary signal: Ecological and environmental factors - Report from Working Group 2. Geochem. Geophys. Geosyst. **2**.

Billings, G. K., O. P. Bricker, Mackenzi.Ft, and A. L. Brooks. 1969. Temporal variation of alkaline earth element/chlorinity ratios in Sargasso Sea. Earth Planet. Sci. Lett. **6:** 231-&.

Bissinger, J. E., D. J. S. Montagnes, J. Sharples, and D. Atkinson. 2008. Predicting marine phytoplankton maximum growth rates from temperature: Improving on the Eppley curve using quantile regression. Limnol. Oceanogr. **53:** 487-493.

Bollmann, J., and J. O. Herrle. 2007. Morphological variation of *Emiliania huxleyi* and sea surface salinity. Earth Planet. Sci. Lett. **255:** 273-288.

Bollmann, J., J. O. Herrle, M. Y. Cortes, and S. R. Fielding. 2009. The effect of sea water salinity on the morphology of Emiliania huxleyi in plankton and sediment samples. Earth Planet. Sci. Lett. **284:** 320-328.

Boye, M., and C. M. G. Van Den Berg. 2000. Iron availability and the release of iron-complexing ligands by Emiliania huxleyi. Mar. Chem. **70:** 277-287.

Brand, L. E. 1981. Genetic variability in reproduction rates in marine phytoplankton populations. Evolution **35:** 1117-1127.

---. 1982. Genetic variability and spatial patterns of genetic differentiation in the reproductive rates of the marine coccolithophores *Emiliania huxleyi* and *Gephyrocapsa oceanica*. Limnol. Oceanogr. **27:** 236-245.

---. 1984. The salinity tolerance of 46 marine-phytoplankton isolates. Estuarine Coastal and Shelf Science **18:** 543-556.

Brand, L. E., and R. R. L. Guillard. 1981. The effects of continuous light and light-intensity on the reproduction rates of 22 species of marine-phytoplankton. J. Exp. Mar. Biol. Ecol. **50:** 119-132.

Brand, L. E., R. R. L. Guillard, and L. S. Murphy. 1981. A method for the rapid and precise determination of acclimated phytoplankton reproduction rates. Journal of Plankton Research **3:** 193-202.

Brass, G. W., and K. K. Turekian. 1972. Strontium distributions in sea-water profiles from GEOSECS-I (Pacific) and GEOSECS-II (Atlantic) test stations. Earth Planet. Sci. Lett. **16:** 117-&.

---. 1974. Strontium distribution in GEOSECS oceanic profiles. Earth Planet. Sci. Lett. **23:** 141-148.

Bucciarelli, E., W. G. Sunda, S. Belviso, and G. Sarthou. 2007. Effect of the diel cycle on production of dimethylsulfoniopropionate in batch cultures of *Emiliania huxleyi*. Aquat. Microb. Ecol. **48:** 73-81.

Buitenhuis, E. T., H. J. W. De Baar, and M. J. W. Veldhuis. 1999. Photosynthesis and calcification by Emiliania huxleyi (Prymnesiophyceae) as a function of inorganic carbon species. J. Phycol. **35:** 949-959.

Buitenhuis, E. T., T. Pangerc, D. J. Franklin, C. Le Quere, and G. Malin. 2008. Growth rates of six coccolithophorid strains as a function of temperature. Limnol. Oceanogr. **53:** 1181-1185.

Buma, A. G. J., T. Van Oijen, W. Van De Poll, M. J. W. Veldhuis, and W. W. C. Gieskes. 2000. The sensitivity of *Emiliania huxleyi* (Prymnesiophycea) to ultraviolet-B radiation. J. Phycol. **36:** 296-303.

Charlson, R. J., J. E. Lovelock, M. O. Andreae, and S. G. Warren. 1987. Oceanic phytoplankton, atmospheric sulfur, cloud albedo and climate. Nature **326:** 655-661.

Chow, T. J., and T. G. Thompson. 1955. Flame photometric determination of strontium in sea water. Analytical Chemistry **27:** 18-21.

Climap. 1981. Seasonal reconstructions of the Earth's surface at the last glacial maximum. Geological Society of America.

Conte, M. H. and others 2006. Global temperature calibration of the alkenone unsaturation index (U-37(K ')) in surface waters and comparison with surface sediments. Geochem. Geophys. Geosyst. **7.**

Conte, M. H., A. Thompson, G. Eglinton, and J. C. Green. 1995. Lipid biomarker diversity in the coccolithophorid *Emiliania huxleyi* (Prymnesiophyceae) and the related species *Gephyrocapsa oceanica*. J. Phycol. **31:** 272-282.

Conte, M. H., A. Thompson, D. Lesley, and R. P. Harris. 1998. Genetic and physiological influences on the alkenone/alkenoate versus growth temperature relationship in Emiliania huxleyi and Gephyrocapsa oceanica. Geochim. Cosmochim. Acta **62:** 51-68.

Cortes, M. Y., J. Bollmann, and H. R. Thierstein. 2001. Coccolithophore ecology at the HOT station ALOHA, Hawaii. Deep-Sea Research Part Ii-Topical Studies in Oceanography **48:** 1957-1981.

Culkin, F., and R. A. Cox. 1966. Sodium, potassium, magnesium, calcium and strontium in sea water. Deep Sea Research **13:** 789-804.

Danbara, A., and Y. Shiraiwa. 1999. The requirement of selenium for the growth of marine coccolithophorids, Emiliania huxleyi, Gephyrocapsa oceanica and Helladosphaera sp (Prymnesiophyceae). Plant and Cell Physiology **40:** 762-766.

De La Cuesta, J. L., and S. L. Manley. 2009. Iodine assimilation by marine diatoms and other phytoplankton in nitrate-replete conditions. Limnol. Oceanogr. **54:** 1653-1664.

De Vernal, A. and others 2001. Dinoflagellate cyst assemblages as tracers of sea-surface conditions in the northern North Atlantic, Arctic and sub-Arctic seas: the new 'n=677' data base and its application for quantitative palaeoceanographic reconstruction. Journal of Quaternary Science **16:** 681-698.

De Villiers, S. 1998. Excess dissolved Ca in the deep ocean: a hydrothermal hypothesis. Earth Planet. Sci. Lett. **164:** 627-641.

---. 1999. Seawater strontium and Sr/Ca variability in the Atlantic and Pacific oceans. Earth Planet. Sci. Lett. **171:** 623-634.

De Villiers, S., and B. K. Nelson. 1999. Detection of low-temperature hydrothermal fluxes by seawater Mg and Ca anomalies. Science **285:** 721-723.

Demicco, R. V., T. K. Lowenstein, and L. A. Hardie. 2003. Atmospheric pCO(2) since 60 Ma from records of seawater pH, calcium, and primary carbonate mineralogy. Geology **31:** 793-796.

Dickinson, R. E., and R. J. Cicerone. 1986. Future global warming from atmospheric trace gases. Nature **319:** 109-115.

Dickson, D., and G. Kirst. 1987a. Osmotic Adjustment in Marine Eukaryotic Algae: The Role of Inorganic Ions, Quaternary Ammonium, Tertiary Sulphonium and Carbohydrate Solutes. II. Prasinophytes and Haptophytes. New Phytol. **106:** 657-666.

Dickson, D. M. J., and G. O. Kirst. 1987b. Osmotic Adjustment in Marine Eukaryotic Algae: The Role of Inorganic Ions, Quaternary Ammonium, Tertiary Sulphonium and Carbohydrate Solutes.I. Diatoms and a Rhodophyte. New Phytol. **106:** 645-655.

Dupont, C. L., R. K. Nelson, S. Bashir, J. W. Moffett, and B. A. Ahner. 2004. Novel copper-binding and nitrogen-rich thiols produced and exuded by Emiliania huxleyi. Limnol. Oceanogr. **49:** 1754-1762.

Dyhrman, S. T., and B. Palenik. 2003. Characterization of ectoenzyme activity and phosphate-regulated proteins in the coccolithophorid *Emiliania huxleyi*. Journal of Plankton Research **25:** 1215-1225.

Elderfield, H., C. J. Bertram, and J. Erez. 1996. Biomineralization model for the incorporation of trace elements into foraminiferal calcium carbonate. Earth Planet. Sci. Lett. **142:** 409-423.

Eppley, R. 1972. Temperature and phytoplankton growth in the sea. Fishery Bulletin **70:** 1063-1085.

Epstein, B. L., S. D'hondt, and P. E. Hargraves. 2001. The possible metabolic role of C-37 alkenones in Emiliania huxleyi. Organic Geochemistry **32:** 867-875.

Evans, C., S. V. Kadner, L. J. Darroch, W. H. Wilson, P. S. Liss, and G. Malin. 2007. The relative significance of viral lysis and microzooplankton grazing as pathways of dimethylsulfoniopropionate (DMSP) cleavage: An Emiliania huxleyi culture study. Limnol. Oceanogr. **52:** 1036-1045.

Evans, C., G. Malin, W. H. Wilson, and P. S. Liss. 2006. Infectious titers of Emiliania huxleyi virus 86 are reduced by exposure to millimolar dimethyl sulfide and acrylic acid. Limnol. Oceanogr. **51:** 2468-2471.

Fabricand, B. P., E. S. Imbimbo, and M. E. Brey. 1967. Atomic absorption analyses for Ca, Li, Mg, K, Rb, and Sr at two Atlantic Ocean stations. Deep Sea Research and Oceanographic Abstracts **14:** 785-788, IN717-IN718, 789.

Fabricand, B. P., E. S. Imbimbo, M. E. Brey, and J. A. Weston. 1966. Atomic Absorption Analyses for Li, Mg, K, Rb, and Sr in Ocean Waters. J. Geophys. Res. **71:** 3917-3921.

Feng, Y. and others 2008. Interactive effects of increased pCO(2), temperature and irradiance on the marine coccolithophore *Emiliania huxleyi* (Prymnesiophyceae). Eur. J. Phycol. **43:** 87-98.

Fernandez, E., J. J. Fritz, and W. M. Balch. 1996a. Chemical composition of the coccolithophorid *Emiliania huxleyi* under light-limited steady state growth. J. Exp. Mar. Biol. Ecol. **207:** 149-160.

Fernandez, E., E. Maranon, and W. M. Balch. 1996b. Intracellular carbon partitioning in the coccolithophorid Emiliania huxleyi. Journal of Marine Systems **9:** 57-66.

Fielding, S. R., J. O. Herrle, J. Bollmann, R. H. Worden, and D. J. S. Montagnes. 2009. Assessing the applicability of *Emiliania huxleyi* coccolith morphology as a sea-surface salinity proxy. Limnol. Oceanogr. **54:** 1475-1480.

Fritz, J. J. 1999. Carbon fixation and coccolith detachment in the coccolithophore Emiliania huxleyi in nitrate-limited cyclostats. Mar. Biol. **133:** 509-518.

Fritz, J. J., and W. M. Balch. 1996. A light-limited continuous culture study of Emiliania huxleyi: Determination of coccolith detachment and its relevance to cell sinking. J. Exp. Mar. Biol. Ecol. **207:** 127-147.

Garde, K., and C. Cailliau. 2000. The impact of UV-B radiation and different PAR intensities on growth, uptake of C-14, excretion of DOC, cell volume, and pigmentation in the marine prymnesiophyte, Emiliania huxleyi. J. Exp. Mar. Biol. Ecol. **247:** 99-112.

Gravalosa, J. M., J. A. Flores, F. J. Sierro, and R. Gersonde. 2008. Sea surface distribution of coccolithophores in the eastern Pacific sector of the Southern Ocean (Bellingshausen and Amundsen Seas) during the late austral summer of 2001. Mar. Micropaleontol. **69:** 16-25.

Green, J. C., B. R. Heimdal, E. Paasche, and R. Moate. 1998. Changes in calcification and the dimensions of coccoliths of Emiliania huxleyi (Haptophyta) grown at reduced salinities. Phycologia **37:** 121-131.

Guan, W. C., and K. S. Gao. 2010. Impacts of UV radiation on photosynthesis and growth of the coccolithophore Emiliania huxleyi (Haptophyceae). Environmental and Experimental Botany **67:** 502-508.

Guillard, R. R. L. 1975. Culture of phytoplankton for feeding marine invertebrates, p. 29-60. *In* W. L. Smith, and M. H. Chanley [ed.], Culture of marine invertebrate animals. Plenum.

Hansson, M. E., and E. S. Saltzman. 1993. The 1st Greenland ice core record of methanesulfonate and sulfate over a full glacial cycle. Geophysical Research Letters **20:** 1163-1166.

Hay, W. W. 2008. Evolving ideas about the Cretaceous climate and ocean circulation. Cretaceous Research **29:** 725-753.

Hay, W. W., A. Migdisov, A. N. Balukhovsky, C. N. Wold, S. Flogel, and E. Soding. 2006. Evaporites and the salinity of the ocean during the Phanerozoic: Implications for climate, ocean circulation and life. Palaeogeography Palaeoclimatology Palaeoecology **240:** 3-46.

Hegseth, E. N., and A. Sundfjord. 2008. Intrusion and blooming of Atlantic phytoplankton species in the high Arctic. Journal of Marine Systems **74:** 108-119.

Henderiks, J., and M. Pagani. 2007. Refining ancient carbon dioxide estimates: Significance of coccolithophore cell size for alkenone-based pCO_2 records. Paleoceanogr. **22**.

---. 2008. Coccolithophore cell size and the Paleogene decline in atmospheric CO_2. Earth Planet. Sci. Lett. **269:** 575-583.

Horibe, Y., K. Endo, and H. Tsubota. 1974. Calcium in South Pacific, and its correlation with carbonate alkalinity. Earth Planet. Sci. Lett. **23:** 136-140.

Houdan, A., I. Probert, K. Van Lenning, and S. Lefebvre. 2005. Comparison of photosynthetic responses in diploid and haploid life-cycle phases of Emiliania huxleyi (Prymnesiophyceae). Mar. Ecol.-Prog. Ser. **292:** 139-146.

Huybrechts, P. 2002. Sea-level changes at the LGM from ice-dynamic reconstructions of the Greenland and Antarctic ice sheets during the glacial cycles. Quaternary Science Reviews **21:** 203-231.

Iglesias-Rodriguez, M. D. and others 2002. Representing key phytoplankton functional groups in ocean carbon cycle models: Coccolithophorids. Global Biogeochem. Cy. **16**.

Iglesias-Rodriguez, M. D. and others 2008. Phytoplankton calcification in a high-CO2 world. Science **320:** 336-340.

Jasper, J. P., and J. M. Hayes. 1990. A carbon stable isotope record of CO_2 levels during the late Quaternary. Nature **347:** 462-464.

Keller, M. D., R. P. Kiene, P. A. Matrai, and W. K. Bellows. 1999a. Production of glycine betaine and dimethylsulfoniopropionate in marine phytoplankton. I. Batch cultures. Mar. Biol. **135:** 237-248.

---. 1999b. Production of glycine betaine and dimethylsulfoniopropionate in marine phytoplankton. II. N-limited chemostat cultures. Mar. Biol. **135:** 249-257.

Kim, S. J., G. M. Flato, and G. J. Boer. 2003. A coupled climate model simulation of the last glacial maximum, Part 2: approach to equilibrium. Climate Dynamics **20:** 635-661.

Kirk, J. 1994. Light and Photosynthesis in Aquatic Ecosystems. Cambridge Univ Pr.

Koenker, R., and G. Bassett. 1978. Regression Quantiles. Econometrica **46:** 33-50.

Krumgalz, B. S., and R. Holzer. 1980. On the determination of Ca-2+ ion concentration in seawater. Limnol. Oceanogr. **25:** 367-370.

Kubilay, N., M. Kocak, T. Cokacar, T. Oguz, G. Kouvarakis, and N. Mihalopoulos. 2002. Influence of Black Sea and local biogenic activity on the seasonal variation of aerosol sulfur species in the eastern Mediterranean atmosphere. Global Biogeochem. Cy. **16**.

Langer, G. and others 2006. Coccolith strontium to calcium ratios in *Emiliania huxleyi*: The dependence on seawater strontium and calcium concentrations. Limnol. Oceanogr. **51:** 310-320.

Langer, G., N. Gussone, G. Nehrke, U. Riebesell, A. Eisenhauer, and S. Thoms. 2007. Calcium isotope fractionation during coccolith formation in Emiliania huxleyi: Independence of growth and calcification rate. Geochem. Geophys. Geosyst. **8**.

Langer, G., G. Nehrke, I. Probert, J. Ly, and P. Ziveri. 2009a. Strain-specific responses of *Emiliania huxleyi* to changing seawater carbonate chemistry. Biogeosciences **6:** 2637-2646.

Langer, G., G. Nehrke, S. Thoms, and H. Stoll. 2009b. Barium partitioning in coccoliths of Emilliania huxleyi. Geochim. Cosmochim. Acta **73:** 2899-2906.

Leal, M. F. C., M. Vasconcelos, and C. M. G. Van Den Berg. 1999. Copper-induced release of complexing ligands similar to thiols by Emiliania huxleyi in seawater cultures. Limnol. Oceanogr. **44:** 1750-1762.

Lecourt, M., D. L. Muggli, and P. J. Harrison. 1996. Comparison of growth and sinking rates of non-coccolith- and coccolith-forming strains of *Emiliania huxleyi* (Prymnesiophyceae) grown under different irradiances and nitrogen sources. J. Phycol. **32:** 17-21.

Lee, K. and others 2006. Global relationships of total alkalinity with salinity and temperature in surface waters of the world's oceans. Geophysical Research Letters **33**.

Legrand, M. 1997. Ice-core records of atmospheric sulphur. Philosophical Transactions of the Royal Society of London Series B-Biological Sciences **352:** 241-250.

Legrand, M., C. Fenietsaigne, E. S. Saltzman, C. Germain, N. I. Barkov, and V. N. Petrov. 1991. Ice-core record of oceanic emissions of dimethylsulfide during the last climate cycle. Nature **350:** 144-146.

Legrand, M. and others 1997. Sulfur-containing species (methanesulfonate and SO4) over the last climatic cycle in the Greenland Ice Core Project (central Greenland) ice core. J. Geophys. Res. **102:** 26663-26679.

Leonardos, N., and G. N. Harris. 2006. Comparative effects of light on pigments of two strains of Emiliania huxleyi (Haptophyta). J. Phycol. **42:** 1217-1224.

Locarnini, R. A., A. V. Mishonov, J. I. Antonov, T. P. Boyer, and H. E. Garcia. 2006. World Ocean Atlas 2005, Volume 1: Temperature. *In* L. S. [ed.], NOAA Atlas NESDIS 62.

Mackenzie, F. T. 1964. Strontium content + variable strontium-chlorinity relationship of Sargasso sea water. Science **146:** 517-&.

Malin, G., and M. Steinke. 2004. Dimethyl sulfide production: what is the contribution of the coccolithophores?, p. 127-164. *In* H. R. Thierstein and J. R. Young [eds.], Coccolithophores: From Molecular Processes to Global Impact. Springer.

Malin, G., S. M. Turner, P. S. Liss, and Aiken. 1992. Sulfur - the plankton climate connection. J. Phycol. **28:** 590-597.

Marlowe, I. T., S. C. Brassell, G. Eglinton, and J. C. Green. 1990. Long-chain alkenones and alkyl alkenoates and the fossil coccolith record of marine sediments. Chem. Geol. **88:** 349-375.

Matrai, P. A., and M. D. Keller. 1994. Total organic sulfur and dimethylsulfoniopropionate in marine-phytoplankton - intracellular variations. Mar. Biol. **119:** 61-68.

Merico, A. and others 2004. Modelling phytoplankton succession on the Bering Sea shelf: role of climate influences and trophic interactions in generating Emiliania huxleyi blooms 1997-2000. Deep-Sea Res. Pt. I **51:** 1803-1826.

Merrett, M. J., L. F. Dong, and N. A. Nimer. 1993. Nitrate availability and calcite production in *Emiliania huxleyi* Lohmann. Eur. J. Phycol. **28:** 243-246.

Mjaaland, G. 1956. Some laboratory experiments on the coccolithophorid *Coccolithus huxleyi.* Oikos **7:** 251-255.

Mohan, R. and others 2008. Ecology of coccolithophores in the Indian sector of the Southern Ocean. Mar. Micropaleontol. **67:** 30-45.

Montagnes, D. J. S., and J. A. Berges. 2004. Determining parameters of the numerical response. Microbial Ecology **48:** 139-144.

Montagnes, D. J. S., J. A. Berges, P. J. Harrison, and F. J. R. Taylor. 1994. Estimating carbon, nitrogen, protein, and chlorophyll-*a* from volume in marine phytoplankton. Limnol. Oceanogr. **39:** 1044-1060.

Montagnes, D. J. S., S. A. Kimmance, and D. Atkinson. 2003. Using Q(10): Can growth rates increase linearly with temperature? Aquat. Microb. Ecol. **32:** 307-313.

Muggli, D. L., and P. J. Harrison. 1996a. EDTA suppresses the growth of oceanic phytoplankton from the Northeast Subarctic Pacific. J. Exp. Mar. Biol. Ecol. **205:** 221-227.

---. 1996b. Effects of nitrogen source on the physiology and metal nutrition of *Emiliania huxleyi* grown under different iron and light conditions. Mar. Ecol.-Prog. Ser. **130:** 255-267.

Muller, A., and P. De Deckker. 2002. Magnesium, calcium and strontium in waters of the southern Tasman Sea at the confluence of the Indian, Pacific and Southern Oceans. Mar. Freshw. Res. **53:** 1115-1128.

Muller, M. N., A. N. Antia, and J. Laroche. 2008. Influence of cell cycle phase on calcification in the coccolithophore Emiliania huxleyi. Limnol. Oceanogr. **53:** 506-512.

Muller, P. J., G. Kirst, G. Ruhland, I. Von Storch, and A. Rosell-Mele. 1998. Calibration of the alkenone paleotemperature index U-37(K ') based on core-tops from the eastern South Atlantic and the global ocean (60 degrees N-60 degrees S). Geochim. Cosmochim. Acta **62:** 1757-1772.

Nagaya, Y., K. Nakamura, and M. Saiki. 1971. Strontium concentrations and strontium chlorinity ratios in sea water of the North Pacific and the adjacent seas of Japan. Journal of the Oceanographical Society of Japan **27:** 20-26.

Naqvi, S. W. A., and C. V. G. Reddy. 1979. Variation in calcium content of the waters of Laccadives (Arabian Sea). Mar. Chem. **8:** 1-7.

Needoba, J. A., and P. J. Harrison. 2004. Influence of low light and a light: Dark cycle on NO3- uptake, intracellular NO3-, and nitrogen isotope fractionation by marine phytoplankton. J. Phycol. **40:** 505-516.

Needoba, J. A., N. A. Waser, P. J. Harrison, and S. E. Calvert. 2003. Nitrogen isotope fractionation in 12 species of marine phytoplankton during growth on nitrate. Mar. Ecol.-Prog. Ser. **255:** 81-91.

Nielsen, M. V. 1997. Growth, dark respiration and photosynthetic parameters of the coccolithophorid Emiliania huxleyi (Prymnesiophyceae) acclimated to different day length-irradiance combinations. J. Phycol. **33:** 818-822.

Nimer, N. A., C. Brownlee, and M. J. Merrett. 1994. Carbon-dioxide availability, intracellular pH and growth-rate of the coccolithophore *Emiliania huxleyi*. Mar. Ecol.-Prog. Ser. **109:** 257-262.

Paasche, E. 1967. Marine plankton algae grown with light-dark cycles. I. *Coccolithus huxleyi*. Physiol. Plant. **20:** 946-&.

---. 1998. Roles of nitrogen and phosphorus in coccolith formation in Emiliania huxleyi (Prymnesiophyceae). Eur. J. Phycol. **33:** 33-42.

---. 1999. Reduced coccolith calcite production under light-limited growth: a comparative study of three clones of *Emiliania huxleyi* (Prymnesiophyceae). Phycologia **38:** 508-516.

---. 2002. A review of the coccolithophorid *Emiliania huxleyi* (Prymnesiophyceae), with particular reference to growth, coccolith formation, and calcification-photosynthesis interactions. Phycologia **40:** 503-529.

Paasche, E., and S. Brubak. 1994. Enhanced calcification in the coccolithophorid *Emiliania huxleyi* (Haptophyceae) under phosphorus limitation. Phycologia **33:** 324-330.

Paasche, E., S. Brubak, S. Skattebøl, J. R. Young, and J. C. Green. 1996. Growth and calcification in the coccolithophorid Emiliania huxleyi (Haptophyceae) at low salinities. Phycologia **35:** 394-403.

Paasche, E., and Klavenes.D. 1970. Physiological comparison of coccolith-forming and naked cells of *Coccolithus huxleyi*. Archiv Fur Mikrobiologie **73:** 143-&.

Pagani, M., J. C. Zachos, K. H. Freeman, B. Tipple, and S. Bohaty. 2005. Marked decline in atmospheric carbon dioxide concentrations during the Paleogene. Science **309:** 600-603.

Page, S., C. R. Hipkin, and K. J. Flynn. 1999. Interactions between nitrate and ammonium in Emiliania huxleyi. J. Exp. Mar. Biol. Ecol. **236:** 307-319.

Pearson, P. N., G. L. Foster, and B. S. Wade. 2009. Atmospheric carbon dioxide through the Eocene-Oligocene climate transition. Nature **461:** 1110-U1204.

Popp, B. N. and others 2006. A new method for estimating growth rates of alkenone-producing haptophytes. Limnology and Oceanography: Methods **4:** 114-129.

Popp, B. N., F. Kenig, S. G. Wakeham, E. A. Laws, and R. R. Bidigare. 1998a. Does growth rate affect ketone unsaturation and intracellular carbon isotopic variability in Emiliania huxleyi? Paleoceanogr. **13:** 35-41.

Popp, B. N., E. A. Laws, R. R. Bidigare, J. E. Dore, K. L. Hanson, and S. G. Wakeham. 1998b. Effect of phytoplankton cell geometry on carbon isotopic fractionation. Geochim. Cosmochim. Acta **62:** 69-77.

Prahl, F. G., and S. G. Wakeham. 1987. Calibration of unsaturation patterns in long-chain ketone compositions for paleotemperature assessment. Nature **330:** 367-369.

Prahl, F. G., G. V. Wolfe, and M. A. Sparrow. 2003. Physiological impacts on alkenone paleothermometry. Paleoceanogr. **18.**

Preunkert, S., B. Jourdain, M. Legrand, R. Udisti, S. Becagli, and O. Cerri. 2008. Seasonality of sulfur species (dimethyl sulfide, sulfate, and methanesulfonate) in Antarctica: Inland versus coastal regions. J. Geophys. Res.-Atmos. **113:** 10.

Price, L. L., K. Yin, and P. J. Harrison. 1998. Influence of continuous light and L : D cycles on the growth and chemical composition of Prymnesiophyceae including coccolithophores. J. Exp. Mar. Biol. Ecol. **223:** 223-234.

Probert, I., and A. Houdan. 2004. The laboratory culture of coccolithophores, p. 217-249. *In* H. R. Thierstein and J. R. Young [eds.], Coccolithophores: From Molecular Processes to Global Impact. Springer.

Raitsos, D. E., S. J. Lavender, Y. Pradhan, T. Tyrrell, P. C. Reid, and M. Edwards. 2006. Coccolithophore bloom size variation in response to the regional environment of the subarctic North Atlantic. Limnol. Oceanogr. **51:** 2122-2130.

Ramos, J. B. E., M. N. Muller, and U. Riebesell. 2010. Short-term response of the coccolithophore *Emiliania huxleyi* to an abrupt change in seawater carbon dioxide concentrations. Biogeosciences **7:** 177-186.

Raven, J. A., and P. G. Falkowski. 1999. Oceanic sinks for atmospheric CO2. Plant Cell Environ. **22:** 741-755.

Rhodes, L. L., B. M. Peake, A. L. Mackenzie, and S. Marwick. 1995. Coccolithophores *Gephyrocapsa oceanica* and *Emiliania huxleyi* (Prymnesiophyceae = Haptophyceae) in New Zealand coastal waters - characteristics of blooms and growth in laboratory culture. New Zealand Journal of Marine and Freshwater Research **29:** 345-357.

Rhodes, R. H., N. a. N. Bertler, J. A. Baker, S. B. Sneed, H. Oerter, and K. R. Arrigo. 2009. Sea ice variability and primary productivity in the Ross Sea, Antarctica, from methylsulphonate snow record. Geophysical Research Letters **36:** 5.

Rickaby, R. E. M. and others 2007. Coccolith chemistry reveals secular variations in the global ocean carbon cycle? Earth Planet. Sci. Lett. **253:** 83-95.

Rickaby, R. E. M., D. P. Schrag, I. Zondervan, and U. Riebesell. 2002. Growth rate dependence of Sr incorporation during calcification of Emiliania huxleyi. Global Biogeochem. Cy. **16.**

Riebesell, U., A. T. Revill, D. G. Holdsworth, and J. K. Volkman. 2000. The effects of varying CO2 concentration on lipid composition and carbon isotope fractionation in Emiliania huxleyi. Geochim. Cosmochim. Acta **64:** 4179-4192.

Riegman, R., W. Stolte, A. a. M. Noordeloos, and D. Slezak. 2000. Nutrient uptake, and alkaline phosphate (EC 3 : 1 : 3 : 1) activity of *Emiliania huxleyi* (Prymnesiophyceae) during growth under N and P limitation in continuous cultures. J. Phycol. **36:** 87-96.

Rogers, W. H. 1992. Quantile regression standard errors. Stata Technical Bulletin **9:** 16-19.

Rohling, E. J. 2000. Paleosalinity: confidence limits and future applications. Marine Geology **163:** 1-11.

---. 2007. Progress in paleosalinity: Overview and presentation of a new approach. Paleoceanogr. **22**.

Rose, J. M., and D. A. Caron. 2007. Does low temperature constrain the growth rates of heterotrophic protists? Evidence and implications for algal blooms in cold waters. Limnol. Oceanogr. **52:** 886-895.

Rost, B., I. Zondervan, and U. Riebesell. 2002. Light-dependent carbon isotope fractionation in the coccolithophorid *Emiliania huxleyi*. Limnol. Oceanogr. **47:** 120-128.

Royer, D. L. 2006. CO2-forced climate thresholds during the Phanerozoic. Geochim. Cosmochim. Acta **70:** 5665-5675.

Royer, D. L., R. A. Berner, and D. J. Beerling. 2001. Phanerozoic atmospheric CO2 change: evaluating geochemical and paleobiological approaches. Earth-Sci. Rev. **54:** 349-392.

Saigne, C., and M. Legrand. 1987. Measurements of methanesulfonic-acid in Antarctic ice. Nature **330:** 240-242.

Saltzman, E. S., P. Y. Whung, and P. A. Mayewski. 1997. Methanesulfonate in the Greenland Ice Sheet Project 2 ice core. J. Geophys. Res. **102:** 26649-26657.

Schmidt, G. A. 1999. Error analysis of paleosalinity calculations. Paleoceanogr. **14:** 422-429.

Schouten, S. and others 2006. The effect of temperature, salinity and growth rate on the stable hydrogen isotopic composition of long chain alkenones produced by Emiliania huxleyi and Gephyrocapsa oceanica. Biogeosciences **3:** 113-119.

Schulz, K. G., B. Rost, S. Burkhardt, U. Riebesell, S. Thoms, and D. A. Wolf-Gladrow. 2007. The effect of iron availability on the regulation of inorganic carbon acquisition in the coccolithophore Emiliania huxleyi and the significance of cellular compartmentation for stable carbon isotope fractionation. Geochim. Cosmochim. Acta **71:** 5301-5312.

Sciandra, A. and others 2003. Response of coccolithophorid *Emiliania huxleyi* to elevated partial pressure of CO2 under nitrogen limitation. Mar. Ecol.-Prog. Ser. **261:** 111-122.

Sen Gupta, R. S., S. Naik, and S. Y. S. Singbal. 1978. Study of fluoride, calcium and magnesium in northern Indian Ocean. Mar. Chem. **6:** 125-141.

Seoane, S., M. Zapata, and E. Orive. 2009. Growth rates and pigment patterns of haptophytes isolated from estuarine waters. J. Sea Res. **62:** 286-294.

Shaked, Y., Y. Xu, K. Leblanc, and F. M. M. Morel. 2006. Zinc availability and alkaline phosphatase activity in Emiliania huxleyi: Implications for Zn-P co-limitation in the ocean. Limnol. Oceanogr. **51:** 299-309.

Shaw, S. L., S. W. Chisholm, and R. G. Prinn. 2003. Isoprene production by Prochlorococcus, a marine cyanobacterium, and other phytoplankton. Mar. Chem. **80:** 227-245.

Sikes, E. L., W. R. Howard, C. R. Samson, T. S. Mahan, L. G. Robertson, and J. K. Volkman. 2009. Southern Ocean seasonal temperature and Subtropical Front movement on the South Tasman Rise in the late Quaternary. Paleoceanogr. **24:** 13.

Simo, R. 2001. Production of atmospheric sulfur by oceanic plankton: biogeochemical, ecological and evolutionary links. Trends in Ecology & Evolution **16:** 287-294.

Sokal, R. R., and F. J. Rohlf. 1995. Biometry, 3rd ed. Freeman.

Sorrosa, J. M., M. Satoh, and Y. Shiraiwa. 2005. Low temperature stimulates cell enlargement and intracellular calcification of coccolithophorids. Mar. Biotechnol. **7:** 128-133.

Steinke, M., G. V. Wolfe, and G. O. Kirst. 1998. Partial characterisation of dimethylsulfoniopropionate (DMSP) lyase isozymes in 6 strains of *Emiliania huxleyi*. Mar. Ecol.-Prog. Ser. **175:** 215-225.

Stoll, H., C. Klaas, I. Probert, J. Ruiz Encinar, and J. Garcia Alonso. 2002a. Calcification rate and temperature effects on Sr partitioning in coccoliths of multiple species of coccolithophorids in culture. Global Planet. Change **34:** 153-171.

Stoll, H. M., J. R. Encinar, J. I. G. Alonso, Y. Rosenthal, I. Probert, and C. Klaas. 2001. A first look at paleotemperature prospects from Mg in coccolith carbonate: Cleaning techniques and culture measurements. Geochem. Geophys. Geosyst. **2.**

Stoll, H. M., Y. Rosenthal, and P. Falkowski. 2002b. Climate proxies from Sr/Ca of coccolith calcite: Calibrations from continuous culture of Emiliania huxleyi. Geochim. Cosmochim. Acta **66:** PII S0016-7037(0001)00836-00835.

Stoll, H. M., and D. P. Schrag. 1998. Effects of Quaternary sea level cycles on strontium in seawater. Geochim. Cosmochim. Acta **62:** 1107-1118.

Stoll, H. M., N. Shimizu, D. Archer, and P. Ziveri. 2007a. Coccolithophore productivity response to greenhouse event of the Paleocene-Eocene Thermal Maximum. Earth Planet. Sci. Lett. **258:** 192-206.

Stoll, H. M., and P. Ziveri. 2004. Coccolithophorid-based geochemical paleoproxies, p. 529-562. *In* H. R. Thierstein and J. R. Young [eds.], Coccolithophores: From Molecular Processes to Global Impact. Springer.

Stoll, H. M., P. Ziveri, M. Geisen, I. Probert, and J. R. Young. 2002c. Potential and limitations of Sr/Ca ratios in coccolith carbonate: new perspectives from cultures and monospecific samples from sediments. Philosophical Transactions of the Royal Society of London Series a-Mathematical Physical and Engineering Sciences **360:** 719-747.

Stoll, H. M., P. Ziveri, N. Shimizu, M. Conte, and S. Theroux. 2007b. Relationship between coccolith Sr/Ca ratios and coccolithophore production and export in the Arabian Sea and Sargasso Sea. Deep-Sea Research Part Ii-Topical Studies in Oceanography **54:** 581-600.

Stolte, W., G. W. Kraay, A. a. M. Noordeloos, and R. Riegman. 2000. Genetic and physiological variation in pigment composition of Emiliania huxleyi (Prymnesiophyceae) and the

potential use of its pigment ratios as a quantitative physiological marker. J. Phycol. **36:** 529-539.

Sunda, W. G., and D. R. Hardison. 2007. Ammonium uptake and growth limitation in marine phytoplankton. Limnol. Oceanogr. **52:** 2496-2506.

Sunda, W. G., R. Hardison, R. P. Kiene, E. Bucciarelli, and H. Harada. 2007. The effect of nitrogen limitation on cellular DMSP and DMS release in marine phytoplankton: climate feedback implications. Aquat. Sci. **69:** 341-351.

Sunda, W. G., and S. A. Huntsman. 1992. Feedback interactions between zinc and phytoplankton in seawater. Limnol. Oceanogr. **37:** 25-40.

Takano, H., R. Takei, E. Manabe, J. G. Burgess, M. Hirano, and T. Matsunaga. 1995. Increased coccolith production by *Emiliania huxleyi* cultures enriched with dissolved inorganic carbon. Applied Microbiology and Biotechnology **43:** 460-465.

Thierstein, H. R., K. R. Geitzenauer, and B. Molfino. 1977. Global synchroneity of late quaternary coccolith datum levels - validation by oxygen isotopes. Geology **5:** 400-404.

Thompson, P. A., and S. E. Calvert. 1995. Carbon-isotope fractionation by *Emiliania huxleyi*. Limnol. Oceanogr. **40:** 673-679.

Thomsen, C., D. E. Schulz-Bull, G. Petrick, and J. C. Duinker. 1998. Seasonal variability of the long-chain alkenone flux and the effect on the U-37(k ')-index in the Norwegian Sea. Organic Geochemistry **28:** 311-323.

Traversi, R. and others 2009. Study of Dome C site (East Antartica) variability by comparing chemical stratigraphies. Microchem J. **92:** 7-14.

Tsunogai, S., M. Nishimura, and S. Nakaya. 1968. Calcium and magnesium in sea water and the ratio of calcium to chlorinity as a tracer of water-masses. Journal of the Oceanographical Society of Japan **24:** 153-159.

Tyrrell, T., and A. Merico. 2004. *Emiliania huxleyi*: bloom observations and the conditions that induce them, p. 75-97. *In* H. R. Thierstein and J. R. Young [eds.], Coccolithophores: From Molecular Processes to Global Impact. Springer.

Vairavamurthy, A., M. O. Andreae, and R. L. Iverson. 1985. Biosynthesis of dimethylsulfide and dimethylpropiothetin by *Hymenomonas carterae* in relation to sulfur source and salinity variations. Limnol. Oceanogr. **30:** 59-70.

Van Bergeijk, S. A., C. Van Der Zee, and L. J. Stal. 2003. Uptake and excretion of dimethylsulphoniopropionate is driven by salinity changes in the marine benthic diatom Cylindrotheca closterium. Eur. J. Phycol. **38:** 341-349.

Van Bleijswijk, J. D. L., R. S. Kempers, M. J. Veldhuis, and P. Westbroek. 1994. Cell and growth characteristics of Type-A and Type-B of *Emiliania huxleyi* (Prymnesiophyceae) as determined by flow-cytometry and chemical analyses. J. Phycol. **30:** 230-241.

Van Bleijswijk, J. D. L., and M. J. W. Veldhuis. 1995. In-situ gross growth-rates of *Emiliania huxleyi* in enclosures with different phosphate loadings revealed by diel changes in DNA content. Mar. Ecol.-Prog. Ser. **121:** 271-277.

Van De Poll, W. H., R. J. W. Visser, and A. G. J. Buma. 2007. Acclimation to a dynamic irradiance regime changes excessive irradiance sensitivity of Emiliania huxleyi and Thalassiosira weissflogii. Limnol. Oceanogr. **52:** 1430-1438.

Van Rijssel, M., and A. G. J. Buma. 2002. UV radiation induced stress does not affect DMSP synthesis in the marine prymnesiophyte *Emiliania huxleyi*. Aquat. Microb. Ecol. **28:** 167-174.

Van Rijssel, M., and W. W. C. Gieskes. 2002. Temperature, light, and the dimethylsulfoniopropionate (DMSP) content of *Emiliania huxleyi* (Prymnesiophyceae). J. Sea Res. **48:** 17 - 27.

Varela, D. E., and P. J. Harrison. 1999. Effect of ammonium on nitrate utilization by Emiliania huxleyi, a coccolithophore from the oceanic northeastern Pacific. Mar. Ecol.-Prog. Ser. **186:** 67-74.

Vasconcelos, M., M. F. C. Leal, and C. M. G. Van Den Berg. 2002. Influence of the nature of the exudates released by different marine algae on the growth, trace metal uptake, and exudation of Emiliania huxleyi in natural seawater. Mar. Chem. **77:** 187-210.

Villa, G., S. Palandri, and S. W. Wise. 2005. Quaternary calcareous nannofossils from Periantarctic basins: Paleoecological and paleoclimatic implications. Mar. Micropaleontol. **56:** 103-121.

Vogt, M. and others 2008. Dynamics of dimethylsulphoniopropionate and dimethylsulphide under different CO2 concentrations during a mesocosm experiment. Biogeosciences **5:** 407-419.

Watabe, N., and K. M. Wilbur. 1966. Effects of temperature on growth calcification and coccolith form in *Coccolithus huxleyi* (Coccolithineae). Limnol. Oceanogr. **11:** 567-&.

Wefer, G., W. H. Berger, J. Bijma, and G. Fischer. 1999. Clues to ocean history: a brief overview of proxies, p. 1-68. *In* G. Fischer and G. Wefer [eds.], Use of Proxies in Paleoceanography: Examples from the South Atlantic. Springer-Verlag.

Weiss, R. F. 1974. Carbon dioxide in water and seawater: the solubility of a non-ideal gas. Mar. Chem. **2:** 203-215.

Wolfe, G. V., S. L. Strom, J. L. Holmes, T. Radzio, and M. B. Olson. 2002. Dimethylsulfoniopropionate cleavage by marine phytoplankton in response to mechanical, chemical, or dark stress. J. Phycol. **38:** 948-960.

Wolff, T. and others 1999. On the reconstruction of paleosalinities, p. 207-228. *In* G. Fischer and G. Wefer [eds.], Use of Proxies in Paleoceanography. Springer Verlag.

Wong, G. T. F., A. U. Piumsomboon, and W. M. Dunstan. 2002. The transformation of iodate to iodide in marine phytoplankton cultures. Mar. Ecol.-Prog. Ser. **237:** 27-39.

Xu, Y., J. M. Boucher, and F. M. M. Morel. 2006. Expression and diversity of alkaline phosphatase ehap1 in *Emiliania huxleyi* (Prymnesiophyceae). J. Phycol. **46:** 85-92.

Young, J. R. 1994. Variation in *Emiliania huxleyi* coccolith morphology in samples from the Norwegian Ehux experiment, 1992. Sarsia **79:** 417-425.

Young, J. R., and P. Ziveri. 2000. Calculation of coccolith volume and its use in calibration of carbonate flux estimates. Deep-Sea Research Part II **47:** 1679-1700.

Zachos, J., M. Pagani, L. Sloan, E. Thomas, and K. Billups. 2001. Trends, rhythms, and aberrations in global climate 65 Ma to present. Science **292:** 686-693.

Zar, J. H. 1999. Biostatistical analysis, 4th ed. Prentice-Hall.

Zeebe, R. E., and D. A. Wolf-Gladrow. 2001. CO_2 in Seawater: Equilibrium, Kinetics, Isotopes. Elsevier.

9 Appendices

9.1 Fielding et al. 2009 Limnol. Oceanogr.

Fielding, S. R., J. O. Herrle, J. Bollmann, R. H. Worden, and D. J. S. Montagnes. 2009. Assessing the applicability of *Emiliania huxleyi* coccolith morphology as a sea-surface salinity proxy. Limnol. Oceanogr. **54:** 1475-1480.

This manuscript provides the basis for Chapter 2. SRF was the primary author; JB, JOH, DJSM, and RHW provided discussion and comments to earlier versions of the manuscript; JB provided plankton data.

9.2 Bollmann et al. 2009 Earth Planet. Sci. Lett.

Bollmann, J., J. O. Herrle, M. Y. Cortes, and S. R. Fielding. 2009. The effect of sea water salinity on the morphology of *Emiliania huxleyi* in plankton and sediment samples. Earth Planet. Sci. Lett. **284:** 320-328.

This manuscript is part of the body of work to which Chapter 2 is related. No part of the manuscript is presented in this thesis as original work. SRF contributed solely to discussion and commented on an earlier version of the manuscript.